SPLIT RING RESONATOR BASED SENSOR FOR MATERIAL CHARACTERIZATION

NEO SHUN YONG

UNIVERSITI TEKNIKAL MALAYSIA MELAKA

SPLIT RING RESONATOR BASED SENSOR FOR MATERIAL CHARACTERIZATION

NEO SHUN YONG

This report is submitted in partial fulfilment of the requirements for the degree of Bachelor of Electronic Engineering with Honours

Faculty of Electronics and Computer Engineering

UNIVERSITI TEKNIKAL MALAYSIA MELAKA

January 2022

DECLARATION

I declare that this report entitled "Spilt Ring Resonator Based Sensor For Material Characterization" is the result of my own research except as cited in the references. The report has not been accepted for any degree and is not concurrently submitted in candidature of any other degree.

Signature : _____ _____

Name : _____NEO SHUN YONG___

Date : _____17-12-2022_____

APPROVAL

I hereby declare that I have checked this report entitled “Spilt Ring Resonator Based Sensor For Material Characterization” and in my opinion, this report it complies the partial fulfillment for awarding the award of the degree of Bachelor of Electronics Engineering with Honours

Signature : _____

Supervisor Name : Mohamad Harris Bin Misran
Pensyarah
Fakulti Kejuruteraan Elektronik Dan Kejuruteraan Komputer
Universiti Teknikal Malaysia Melaka (UTeM)
Hang Tuah Jaya
76100 Durian Tunggal, Melaka

Date :

ABSTRACT

In these few years, measuring the electromagnetic properties of materials has important applications in many fields due to its wide application in all walks of life in today's material characterization research. In this project, split ring resonator (SRR) are proposed to measure the permittivity of small samples of unknown materials. Strikingly, measuring the electromagnetic properties of materials technology has matured and has undergone multi-faceted investigations. Many industries require accurate material characterization tools, such as the food industry, quality control, chemical composition analysis, and biological sensing. These accurate instruments have the ability to understand the characteristics of materials based on chemical, physical, magnetic and electrical composition characteristics. However, these types of sensors have various well-known limitations, including high manufacturing costs due to complex design structures and large sizes. Consequently, the design of the split ring resonator was introduced and investigated to accurately measure the material performance characterization. Through different offset resonant frequencies instead of a single frequency and polynomial fitting method, the proposed sensor can accurately calculate the unknown dielectric constant. In addition, find out a suitable shape of split ring resonator by studying split ring resonators of different shapes. The resonant frequency of simulation and experiment is 3.5GHz will verify the effectiveness of the proposed method and design. Various standard dielectrics test the sensitivity of the material under test (such as Roger 5880, Roger 4350, Roger 3010 and FR4) to verify that it is a promising low-cost, compact size, easy-to-manufacture and small MUT that can be used in applications that require new sensing technology for quality and control industries.

ABSTRAK

Dalam beberapa tahun ini, mengukur sifat elektromagnet bahan mempunyai aplikasi penting dalam banyak bidang kerana aplikasinya yang meluas dalam semua lapisan masyarakat dalam penyelidikan pencirian bahan hari ini. Dalam projek ini, resonator cincin belah (SRR) dicadangkan untuk mengukur kebolehtelapan sampel kecil bahan yang tidak diketahui. Secara mengejutkan, mengukur sifat elektromagnet teknologi bahan telah matang dan telah melalui penyiasatan pelbagai aspek. Banyak industri memerlukan alat pencirian bahan yang tepat, seperti industri makanan, kawalan kualiti, analisis komposisi kimia dan penderiaan biologi. Instrumen yang tepat ini mempunyai keupayaan untuk memahami ciri bahan berdasarkan ciri komposisi kimia, fizikal, magnet dan elektrik. Walau bagaimanapun, jenis penderia ini mempunyai pelbagai batasan yang terkenal, termasuk kos pembuatan yang tinggi disebabkan oleh struktur reka bentuk yang kompleks dan saiz yang besar. Akibatnya, reka bentuk resonator cincin belah telah diperkenalkan dan disiasat untuk mengukur dengan tepat pencirian prestasi bahan. Melalui frekuensi resonans offset yang berbeza dan bukannya kaedah pemasangan frekuensi tunggal dan polinomial, sensor yang dicadangkan boleh mengira dengan tepat pemalar dielektrik yang tidak diketahui. Di samping itu, ketahui bentuk resonator cincin belah yang sesuai dengan mengkaji resonator cincin belah yang berlainan bentuk. Kekerapan resonan simulasi dan eksperimen ialah 3.5GHz akan mengesahkan keberkesanan kaedah dan reka bentuk yang dicadangkan. Pelbagai dielektrik standard menguji kepekaan bahan yang sedang diuji (seperti Roger 5880, Roger 4350, Roger 3010 dan FR4) untuk mengesahkan bahawa ia adalah kos rendah yang menjanjikan, saiz padat, mudah dibuat dan MUT kecil yang boleh digunakan dalam aplikasi yang memerlukan teknologi penderiaan baharu untuk industri kualiti dan kawalan.

ACKNOWLEDGEMENT

First of all, I would like to express my sincere appreciation to my project supervisor, Dr. Mohamad Harris Misran, who has invested his full effort and time in guiding me in achieving the objectives of the project. His guidance and knowledge has helped me to complete this project. He provided a lot of guidance to solve any problem that occurs throughout this project. Without Dr. Harris as my supervisor, I may not solve the problem that occurs in the project hence cannot complete the project on time. He was also concerns about the progress of my project and gives me support.

Next, I want to show my appreciation to my parents and family who are always support me from beginning of the project until completing the project. This project helped me to gain many things like understanding, patience and support in order to finish my project.

Last but not least, I would also like to express my appreciation to Universiti Teknikal Malaysia Melaka (UTeM), Faculty of Electronics and Computer Engineering for giving me this opportunity for doing this project. Besides that, I would like to thank my friends and seniors for giving me their advice and opinion to complete this project.

TABLE OF CONTENTS

DECLARATION i
APPROVAL ii
ABSTRACT iii
ABSTRAK iv
ACKNOWLEDGEMENT v
TABLE OF CONTENTS vi
LIST OF TABLES viii
LIST OF FIGURES ix
LIST OF SYMBOLS AND ABBREVIATIONS xi
LIST OF APPENDICES xii
INTRODUCTION 1
1.1 Project Background 1
1.2 Problem Statement 2
1.3 Objective 2
1.4 Scope 2
1.5 Thesis Outline 3
LITERATURE REVIEW 5
2.1 Introduction 5
2.2 Instrumentation 5
2.2.1 SMA Port 6
2.2.2 FR 4 6
2.2.3 Roger 5880 and 5870 7
2.2.4 Roger 4350 8
2.2.5 Roger 3010 9
2.2.6 China Made High Frequency Substrate F4B 10
2.2.7 Comparison Between Fr-4 And Rogers 10
2.3 Measurement Methods 11
2.3.1 Transmission/ Reflection Line Method 13
2.3.2 Open Ended Coaxial Probe Method 13
2.3.3 Free Space Method 14
2.3.4 Resonant Method (Cavity) 14

2.3.5 Comparison Between Measuremnt Methods 15
2.4 Antenna Parameters 16
2.4.1 Return Loss 17
2.4.2 Input Impedance 17
2.4.3 Bandwidth 18
2.4.4 Gain 18
2.4.5 Polarization 18
2.5 Resonant Frequency 19
2.6 Research of Split Ring Resonator 20
2.7 Summary 22
METHODOLOGY 23
3.1 Introduction 23
3.2 Research Methodology 24
3.2.1 Work Flow Block Diagram 24
3.2.2 Metamaterials Split Ring Resonators SRR 25
The hexagonal SRR's Resonant Frequency can be calculated using the equation. 26
3.2.3 Overall Project Methodology 27
3.3 Software Used 27
3.3.1 CST Microwave Studio 28
3.4 Design of SRR 29
3.4.1 SRR Resonant Frequency 30
3.4.2 Materials Used 31
3.5 Resonant Cavity Method 32
3.6 Split Ring Resonator (FR-4) Fabrication 32
3.6.1 Printing the Design of Split Ring Resonator 32
3.6.2 Removing the Unwanted Copper 33
3.6.3 Drying 34
3.6.4 Cutting 34
3.6.5 Soldering 35
3.7 Summary 35
RESULT AND DISCUSSION 37
4.1 Introduction 37

4.2 Resonant Frequency of Three Different Shape of Split Ring Resonator 37
4.3 Fabricated Antenna 39
4.3.1 CST Design 39
4.3.2 Fabricated Design 39
4.4 Resonant Frequency of Different Gap 40
4.5 Parameter List of Split Ring Resonator 40
4.6 Comparison Resonant Frequency and Shift Frequency Between Different Dielectric Constant 42
4.7 Result of Split Ring Resonator 45
4.7.1 Measure the split ring resonator in lab microwave 45
4.7.2 Simulation and Measurement of Split Ring Resonator 46
4.7 Discussion 48
4.8 Summary 50
CONCLUSION AND RECOMMENDATION 51
5.1 Conclusion 51
5.2 Recommendation for Future Work 52
REFERENCES 53
APPENDICES 56
Appendix A: LIST OF DIELECTRIC MATERIALS AND PROPERTIES 56
Appendix B: FR-4 DATA SHEET 57
Appendix C: ROGER 5870 AND 5880 DATA SHEET 58
Appendix D: ROGER 4003C AND 4390B DATA SHEET 59
Appendix E: CHINA MADE HIGH FREQUENCY SUBSTRATE F4B DATA SHEET 60
Appendix F: ROGER 3010 DATA SHEET 61

LIST OF TABLES

TABLE	TITLE	PAGE
Table 1	Dielectric Constans of Rubber and Polymer Materials	12
Table 2	Advantages and limitations of each technique	16
Table 3	Research of Split Ring Resonator	21

Table 4	The specifications of used SUT materials for sensing	31
Table 5	Gantt Chart of FYP 1	36
Table 6	Gantt Chart of FYP 2	36
Table 7	Parameter List of Split Ring Resonator	41
Table 8	Resonant Frequency and Shift Frequency of Different Dielectric Constant	42

LIST OF FIGURES

FIGURE	TITLE	PAGE
Figure 2.2	Location of measured SUT on the designed sensor	5
Figure 2.2.1	SMA Port	6
Figure 2.2.2	FR-4	6
Figure 2.2.3.1	Roger 5880 and 5870	7
Figure2.2.3.2	Roger 5880	8
Figure 2.2.4	Roger 4350	8
Figure 2.2.5	Roger 3010	9
Figure 2.2.6	China Made High Frequency Substrate F4B	10
Figure 2.2.7	Comparison between FR-4 and Rogers RO4350	10
Figure 2.3.1	Transmission/ Reflection measurement method based on coxial line	13
Figure 2.3.2	Use an open coaxial probe to measure tissue samples	14
Figure 2.3.3	Use the free space method to measure samples	14
Figure 2.3.4	Measuring thin films using cavity resonators	15

Figure 2.4.1	Return Loss	17
Figure 2.5	Resonant frequency with dielectric constant for different substrate values	20
Figure 3.2.2.1	Size of Circular Ring	25
Figure 3.2.2.2	Size of Square Ring	25
Figure 3.2.2.3	Size of Hexagonal Ring	26
Figure 3.2.3	Flowchart of Methodology	27
Figure 3.3.1	Split Ring Resoantor design in CST	28
Figure 3.4a	Square Split Ring Resonator	29
Figure 3.4b	Circular Split Ring Resonator	29
Figure 3.4c	Hexagonal SRR	29
Figure 3.4.1	Equivalent circuit of the SRR show in Figure 3.4	30
Figure 3.6.1	Exposure Machine	33
Figure 3.6.2	Striping	34
Figure 3.6.3	Drying Machine	34
Figure 3.6.4.1	Bottom View	34
Figure 3.6.4.2	Top View	34
Figure 3.6.5	Split Ring Resonator After Soldering	35
Figure 4.2.1(a)	C-SRR	38
Figure 4.2.1(b)	S-SRR	38
Figure 4.2.1(c)	H-SRR	38
Figure 4.2.2	Comparison of S-parameters between different shape, ring width and diameter of SRR	38
Figure 4.3.1(a)	Front design of SRR in CST	39

Figure 4.3.1(b)	Back design of SRR in CST	39
Figure 4.3.2(a)	Front design of SRR after fabricate	39
Figure 4.3.2(b)	Back design of SRR after fabricate	39
Figure 4.4.1	Comparison of S-parameters between different shape and split gap dimension of SRR	40
Figure 4.5	Circular Split Ring Resonator	41
Figure 4.6.1	Resonant frequency of different dielectric constant	43
Figure 4.6.2	Shift frequency of different dielectric constant	44
Figure 4.6.3	Resonant frequency of different material under test (MUT)	44
Figure 4.7.1.1	Split ring resonator based sensor test MUT by network analyzer	45
Figure 4.7.1.2	Split ring resonator with test cable	45
Figure 4.7.1.3	Material under test on split ring resonator	45
Figure 4.7.2.1	Comparison between simulation of FR-4 and air	46
Figure 4.7.2.2	Comparison between measurement of FR-4 and air	46
Figure 4.7.2.3	Comparison between measurement and measurement of FR-4 and air	47
Figure 4.7.2.4	Dielectric constant of shift frequency -0.08	47

LIST OF SYMBOLS AND ABBREVIATIONS

BW - Bandwidth

C - Capacitor

C-SRR - Circular Split Ring Resonator

dB - Decibel

DC - Dielectric Contant

H - Magnetic Field

HF - High Frequency

H-SRR - Hexagon Split Ring Resonator

L - Inductor

MUT - Material Under Test

MW - Microwave

SRR - Split Ring Resonator

S-SRR - Square Split Ring Resonator

SUT - Sample Under Test

μ - Permeability

λ - Wavelength

LIST OF APPENDICES

APPENDIX	TITLE	PAGE
APPENDIX A	List of Dielectric Materials and Properties	56
APPENDIX B	FR-4 DATA SHEET	57
APPENDIX C	ROGER 5870 AND 5880 DATA SHEET	58
APPENDIX D	ROGER 4003C AND 4390B DATA SHEET	59
APPENDIX E	CHINA MADE HIGH FREQUENCY SUBSTRATE F4B DATA SHEET	60
APPENDIX F	ROGER 3010 DATA SHEET	61

CHAPTER 1

INTRODUCTION

1.1 Project Background

In the recent years, the usage of microstrip antenna has keep increasing all around world. This is because microstrip antennas have been widely used in satellite communications, radar, remote sensing, missiles, environmental testing, portable wireless equipment and other fields. As a developing country, the Malaysian government provides support and encouragement in terms of development sources to improve the technological development of Malaysian microstrip antennas. In Malaysia, wireless devices play an indispensable and important role in people's lives. With the rapid development of microwave circuit technology that can accurately measure the complex permittivity of materials, it plays an important role in microwave applications. The most important thing to characterize a material is to understand its composition and material properties related to physical, chemical, magnetic, and electrical properties. Permittivity is an important parameter describing the electromagnetic properties of dielectric materials. Dielectric materials are materials that do not conduct electricity, such as glass and ceramics. Different types of materials have their own dielectric constants. The most common sensors on the market have high Q factors and sensitivity, but these types of sensors have various well-known limitations, including high manufacturing costs due to complex design structures and large sizes. These limitations associated with conventional devices are subjective and have therefore led to the proposed split ring resonator because it has the advantages and disadvantages of being compact in size, simple, easy to manufacture, and minimizing the manufacturing cost of manufacturing them. In this work, a split ring resonator (SRR) based sensor used in the ground plane for dielectric measurement is proposed. This method allows for simultaneous assessment of relative permittivity and relative permeability, as well as a straightforward sample preparation procedure. The SRR's design, simulation, and prediction equations are the core of this research.

1.2 Problem Statement

The split ring resoantor has negative permeability in a certain frequency band, and can form a band gap in the working frequency band of the split ring resonator. Using this feature in the split ring resonator can effectively suppress the surface waves and parasitic radiation excited by the split ring resonator when it works. .

Next, the limitations existing in traditional split ring resonator in terms of complexity, size, cost, sentivity and can only work effectively in a certain frequency band. This greatly limits the application prospects of split ring resonator. Based on this problem, it is of course necessary to develop a simpler split ring resonator with low-cost, highly sensitive and easier to manufacture.

1.3 Objective

The objectives of this project are:

- To design a split ring resonator sensor for accurate complex permittivity measurements of solid dielectrics.
- To determine the relationship between resonant frequency and complex permittivity of materials.
- To verify the simulation result using lab measurement.

1.4 Scope

In order to achieve the objectives of the project, aiming at the narrow band and low efficiency of microstrip antennas to design a new type of split ring resonator microstrip antenna with wide frequency band, high gain, small size and simple structure. By introducing a narrower bandwidth to provide higher sensitivity, which helps compared with the traditional SRR design, it has a higher Q factor.

The method of loading a metal split resonant ring can be applied to the transformation of microstrip antennas in various occasions. Developed for material characterization in various frequency bands which includes transmission-line, free-space, open ended coaxial probe, resonant cavity methods, and select appropriate measurement methods. This project involves the software of CST studio suite to simulate and analysis the resonant frequency of different design of split ring resonator and comparison it.

1.5 Thesis Outline

This thesis consists of five chapters which are introduction, literature review, methodology, result & analysis and conclusion & recommendation.

In Chapter 1, it discuss about brief introduction of this project which include project background, problem statement, objective, scope and thesis outlines. These chapters also discuss about the advantages of the split ring resonator (SRR).

In Chapter 2, it discuss about the literature review of this project. This chapter include the explanation about experimental data and the reflection coefficients under various dielectric constant of SUTs. The theory of split ring resoantor also describe in this chapter. For completing this project, all the journals and books that related to this project are used as a references.

In Chapter 3, it discuss about the methodology of the project. The project activity is to describe the flow of the whole project which stated in the project flowchart. All the method and procedure used in completing the project is explained in this chapter. There are some important method like sensing algorithms and testing split ring resonator in software CST microwave studio.

In Chapter 4, it discuss about the result and analysis. This chapter was present all the data and results of the project. The discussion of the result about this project was be stated in this chapter.

In Chapter 5, it discuss about the conclusion of this project and the recommendation for other researcher. It conclude all the topics that have been realized in previous chapters. Besides that, some recommendation are written for the future improvement.

CHAPTER 2

LITERATURE REVIEW

2.1 Introduction

In this chapter, it discuss about all the theories and literature reviews of the Split Ring Resonator. The content of this chapter include introduction of FR 4, SMA port, Roger 5870, Roger 5880, Roger 4350 and some theories magnetic materials.

2.2 Instrumentation

The component used in this project are SMA port, Fr 4, Roger 4350, Roger 5880 and other parts.

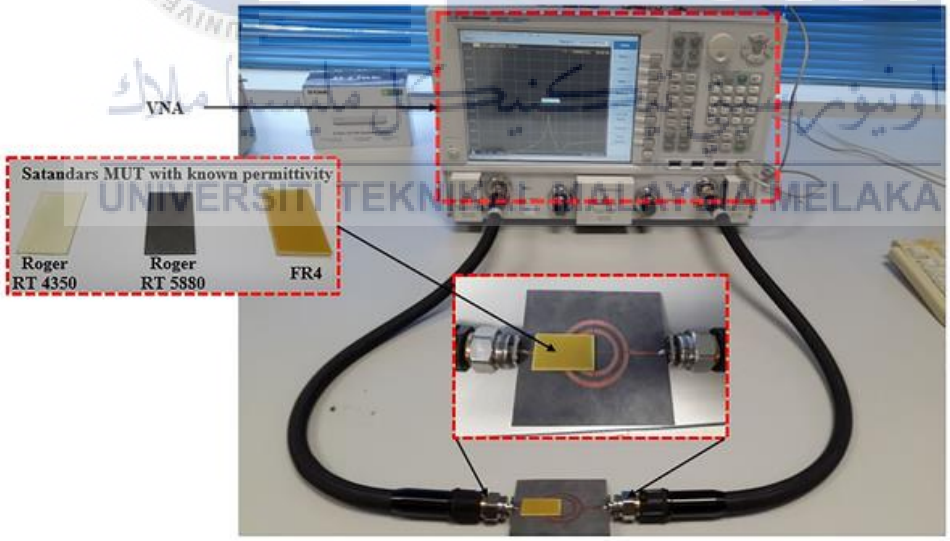

Figure 2.2: Location of measured SUT on the designed sensor

2.2.1 SMA Port

Figure2.2.1：SMA Port

SMA connector is a widely used semi-precision subminiature radio frequency and microwave connector, especially suitable for radio frequency connection in electronic systems with frequencies up to 18GHz or higher. There are many types of SMA connectors, male, female, straight, right-angle, bulkhead connectors, etc., which can meet most requirements. Its ultra-compact size also makes it usable, even in relatively small electronic devices.

Although it is very mature now, SMA connectors are likely to expand their range of use, because many new radio frequency systems extend their operating frequencies to the microwave region. Although SMA connectors resemble common household connectors used for home satellite TV and other related purposes, they are not interchangeable. F-type coaxial connectors, with a 75 ohm impedance, are common household connectors. They have differing diameters and can't be used with SMA connectors without a special adapter, resulting in an impedance mismatch.

2.2.2 FR 4

Figure 2.2.2: FR-4

Glass-reinforced epoxy resin laminates are designated as FR-4 by NEMA. FR-4 is a flame-retardant composite material made out of woven glass fibre fabric and an epoxy resin glue. The term "flame retardant" does not imply that a material meets the UL94V-0 standard unless it has been evaluated in a compliance laboratory using the UL 94 vertical burning test described in section 8.

The high-pressure thermosetting plastic laminate grade FR-4 glass epoxy resin has a strong strength-to-weight ratio and is widely used. Because of its low water absorption, FR-4 is most typically employed as an electrical insulator with high mechanical strength. This material's high mechanical value and electrical insulation capabilities are widely known in both dry and wet environments. This grade's properties, as well as its good production capabilities, make it appropriate for a wide range of electrical and mechanical applications. Bromine (a halogen) is commonly used in FR-4 epoxy resin systems to increase the flame retardancy of FR-4 glass epoxy laminates.

2.2.3 Roger 5880 and 5870

Figure 2.2.3.1: Roger 5880 and 5870

Roger 5880 laminate it is suited for high-frequency/broadband applications because it has a low dielectric constant (Dk) and minimal dielectric loss. The randomly aligned microfibers that strengthen the PTFE composite help to maintain Dk homogeneity.

- Dk or 2.20 +/- .02
- The dissipation factor at 10GHz is 0.0009
- Low moisture absorption
- Isotropic

Roger 5870 and 5880 glass microfiber-reinforced PTFE composites are specifically designed for strict stripline and microstrip circuit applications. Randomly oriented microfibers result in excellent dielectric constant uniformity. The dielectric constant of Roger 5870 and 5880 laminates is uniform from panel to panel and remains constant over a wide frequency range. Its low loss factor extends the use of Roger 5870 and 5880 laminates to the Ku band and beyond. Roger 5870 and 5880 laminates are easy to cut, cut and process. They are resistant to all solvents and reagents, whether hot or cold, and are usually used to etch printed circuits or plate edges and holes. Roger 5870 and 5880 composites are usually supplied in the form of laminates of 0.5 to 2 ounces per foot of electrodeposited copper or reverse-treated EDC, or they can be covered with rolled copper foil for more critical electrical applications. It can also be specified with aluminum, copper or brass plates for cladding.

Figure 2.2.3.2: Roger 5880

2.2.4 Roger 4350

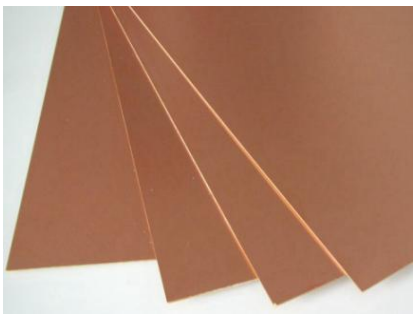

Figure 2.2.4: Roger 4350

Roger 4350 is a flame-retardant version of Roger 4003. Compared with PTFE type, both laminates have better rigidity, which is the same as FR4. Rogers 4350 PCB material is a thermosetting material filled with hydrocarbon/glass reinforced ceramics with a high glass transition temperature (TG> 280℃). Roger 4350 is designed to provide the best RF (radio frequency) performance and the most cost-effective circuit production. Rogers 4350 high frequency material is a ceramic laminate, designed for large capacity and high performance in commercial applications. These series of laminates can be easily converted into printed circuits using standard FR4 board processing technology. It does not require special preparation. Roger 4350 dielectric constant, the temperature coefficient of dielectric constant is one of the lowest among all PCBs. In addition, the dielectric constant is stable over a wide frequency range. Ideal for broadband applications.

2.2.5 Roger 3010

Figure 2.2.5: Roger 3010

Roger 3010 is a ceramic-filled PTFE composite or laminate with a frequency range of up to 77 GHz. With a dielectric constant of 11.20 to 40 GHz at normal temperature, it exhibits outstanding electrical and mechanical stability. At 10 GHz, the material has a loss factor of 0.0022, making it ideal for applications such as car radar, GPS antennas, patch antennas, and direct broadcast satellites.

2.2.6 China Made High Frequency Substrate F4B

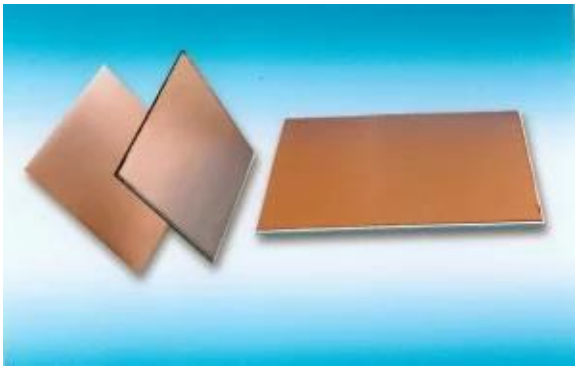

Figure 2.2.6: China Made High Frequency Substrate F4B

F4B high-frequency materials mainly include PTFE fiber glass cloth and ceramic-filled PTFE fiber glass cloth. It is a substrate of high-frequency materials of Chinese brands with low price and stable quality. It is widely used in satellite communications, navigation, radar, 4G communications, 5G communications and other fields. The main specification of this board is double-sided, the substrate is F4B, the DK is 2.2, the finished copper is 1.0oz, no solder mask or silk screen, and the surface treatment is OSP. The top and bottom layers are 1oz copper finished products. The F4b dielectric material is located between the two layers of copper, with a dielectric constant of 2.2 and a thickness of 3.0mm. The dielectric constant of F4B material is relatively wide, ranging from 2.2 to 3.0. The board thickness ranges from 0.17mm to 5.0mm.

2.2.7 Comparison Between Fr-4 And Rogers

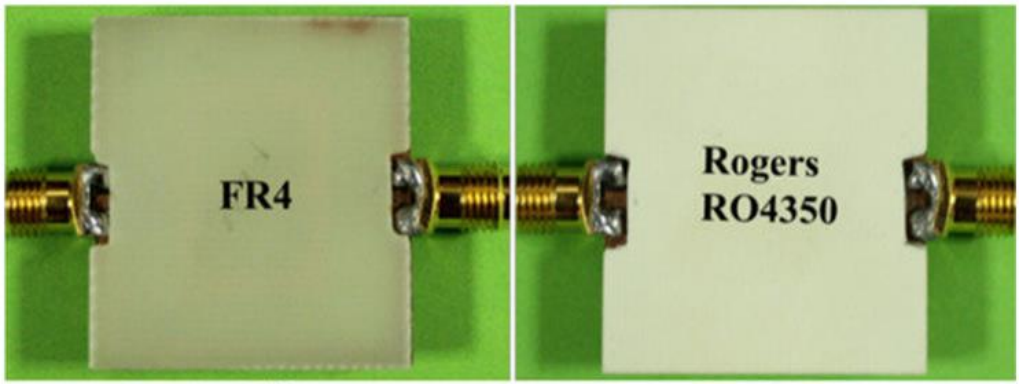

Figure 2.2.7 : Comparison between FR-4 and Rogers 4350

Each material has its own advantages and disadvantages. Compared with rogers, fr-4 is cheaper than rogers, and has a higher Df or loss factor than Roger, and suffers more signal loss. On the other hand, compared with fr-4, rogers material performs well in high frequency. In terms of impedance stability, Rogers' Dk value range is wider than fr-4. For the dielectric constant, the dk of fr-4 is about 4.5, which is lower than that of rogers about 6.15 to 11. In terms of temperature management, rogers has a smaller change compared with fr-4 material.

Fr-4 provides a basic standard for PCB substrates, maintaining a broad and effective balance between cost, durability, performance, manufacturability, and electrical characteristics. However, because performance and electrical characteristics play an important role in your design, rogers has the following advantages: low electrical signal loss, effective PCB manufacturing cost, lower dielectric loss, better thermal management, dk (medium The electric constant) has a wide range of values, 2.55-10.2, low outgassing for space applications and improved impedance control.

2.3 Measurement Methods

Previous dielectric studies employed a variety of measuring methodologies, this section introduces and briefly discusses the most commonly used methods. The dielectric constant and complex relative permeability of materials with complex relative values are measured when dielectric characteristics are measured. A real part and an imaginary part make up complicated permittivity. The permittivity, also known as the real part of the complex permittivity, is a measure of the external electric field energy stored in the material. The imaginary portion, often known as the loss factor, is a lossless material having a value of 0. This is the energy that the material loses as a result of the external electric field. The loss tangent denotes the ratio of the complex permittivity's imaginary and real parts. Only magnetic materials can have their complicated permeability measured. Due to the non-magnetic nature of most materials, their permeability is very near to that of free space. In Table 1 was show the dielectric constant of some sample materials in 9.6 GHz. The use of VNA as a flexible and versatile tool to accurately and quantitatively characterize material properties in the range from a few KHz to THz has been discussed, such as permittivity and permeability. Different methods have been proposed to

extract the permittivity and permeability of the MUT from 2-port or 1-port S-parameter measurements. The types of MUT that can be characterized using VNA range from biological substances, liquids to solids and powders, highlighting the wide applicability of VNA as a tool for characterizing high-frequency materials. There are many methods developed for measuring the complex permittivity and permeability. Transmission/reflection line method, open ended coaxial probe method, free space method and resonant method were discussed in following section.

Table 1: Dielectric Constans of Rubber and Polymer Materials

Sample Material	Dielectric Constant (ε_r) in 9.6 GHz
NR	4.6015
IIR	3.4780
BIIR	4.0540
NBR	2.7541
HNBR	3.2462
SBR	4.3860
SBR-1958	5.0261
SBR-1502	4.5275
CSM	2.6050
Silicone Rubber	4.8272
Reclaim Rubber	3.5213
RSS	3.8710
Brown Crepe Rubber	3.7215
PET	5.9230
HDPE	4.9225

ABS	5.6624
Nylon 66	4.6620
GF NYLON 66	6.5615

2.3.1 Transmission/ Reflection Line Method

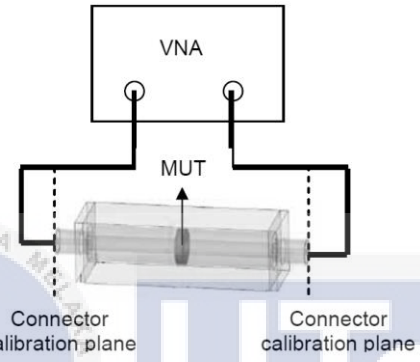

Figure 2.3.1: Transmission/ Reflection measurement method based on coxial line

The MUT is placed in a coaxial line, or in the case of anisotropic tissue, in a rectangular waveguide, so that the field polarisation can be altered in the transmission line measuring method. The scattering parameters S21 and S11 are obtained by connecting the transmission line to the VNA's two ports, and then transformed into the tissue's complicated dielectric constant dielectric characteristics.

2.3.2 Open Ended Coaxial Probe Method

Many of the limitations associated with the above-mentioned technique are not present in the coaxial probe technology. The open coaxial probe is made up of a section of the transmission line that has been broken off. The electromagnetic field travels along the coaxial connection, and when it comes into contact with an impedance mismatch between the probe and the tissue sample, it reflects. Figure 2 depicts the open coaxial probe measuring equipment and probe cross section. Measure the reflected signal at various frequencies and convert it to a complex permittivity value.

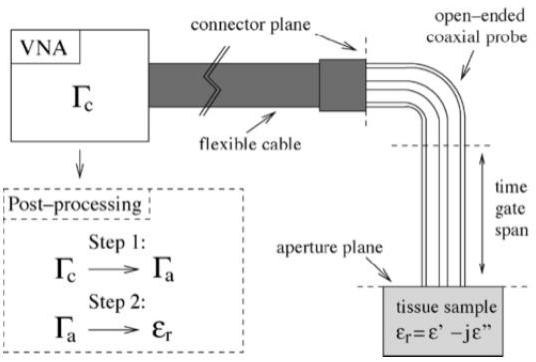

Figure 2.3.2 : Use an open coaxial probe to measure tissue samples

2.3.3 Free Space Method

At microwave frequencies, a non-destructive free-space approach for measuring the complex permittivity of double-layer dielectrics and thin-film oxide layers has been devised. Free space methods, which often operate at broadband frequencies, can be used in high-temperature or severe situations. The SUT must be large and flat in order to be used for this measurement. In the 18-26 GHz range, this approach uses a vector network analyzer and a point-focused antenna system.

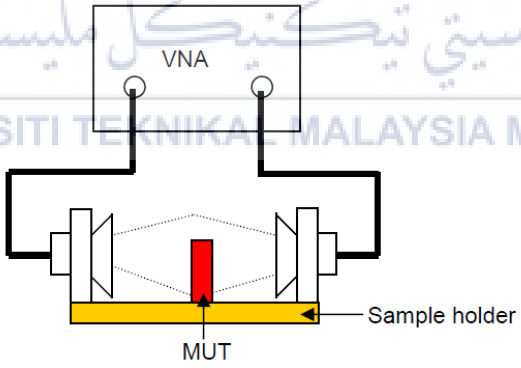

Figure 2.3.3 : Use the free space method to measure samples

2.3.4 Resonant Method (Cavity)

A square patch antenna-based dielectric constant resonant method is used to characterize the real part of the dielectric constant. This method uses FR4 substrates with known dielectric

properties for verification. Finally, various tasks are performed to further verify and test the accuracy of the proposed method.

Resonance measurement is the most accurate method to obtain dielectric constant and permeability. When it is necessary to accurately understand the electromagnetic properties of a material at a specific frequency or multiple discrete frequencies, resonance technology can be used. However, the frequency and loss characteristics of materials that can be measured by this method are limited. There are many types of resonance methods available, such as cavity, split cylindrical resonator, cavity resonator, Fabry-Perot resonator, and so on.

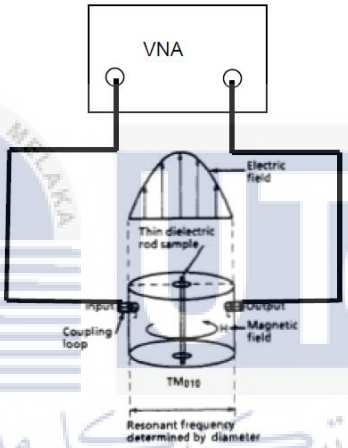

Figure 2.3.4: Measuring thin films using cavity resonators

2.3.5 Comparison Between Measuremnt Methods

Each method has its own field of application, and the best choice depends on the frequency range of interest, the required measurement accuracy, isotropy and homogeneity, form (ie powder, liquid, solid), size, non-destructive or non-destructive requirements. Non-contact testing and temperature range. The following table 2 summarizes the advantages, scope and limitations of each techniques.

Table 2 : Advantages and limitations of each technique

Measurement Techniques	Open-end coaxial probe	Transmission line	Free space	Resonant method (Cavity)
Advantages	After calibration, the dielectric properties of a large number of samples can be measured in a short time.	The dielectric constant and permeability of the substrate under test (SUT) can be determined.	Can use for HF measurement and allows non-destructive measurement.	Can measure very small MUT.
Disadvantages	-Air gap effects limited the accuracy of measurement. - Limited to low accuracy	- Measurement on specimen will be affected by air gap.	-Multiple reflections between the antenna and the sample surface. - Edge of sample effected by diffraction.	-VNA that requires HF resolution -Limited to narrowband frequencies.
S- Parameters	S_{11}	S_{11}, S_{12}	S_{11}, S_{12}	Resonant Frequency, Q-Factor
Dielectric Properties	ε_r	ε_r, μ_r	ε_r, μ_r	ε_r, μ_r
Capabilities & Limitations	• Broadband • port only • Low Accuracy	• Brandband • Best for lossy to low loss	• Broadband • Contactless • Alignment issues • Multiple reflections	• High accuracy • Single frequency • Low loss or thin samples

2.4 Antenna Parameters

Understanding important antenna parameters is critical for choosing and using antennas in almost any application. Return loss (S11), input impedance, bandwidth , gain and polarisation are all metrics that can be used to estimate an antenna's efficiency.

2.4.1 Return Loss

The Return Loss of an antenna is the percentage of radio waves arriving at the antenna input that are rejected in comparison to those that are accepted. When the operating frequency is below -10dB of S12, an antenna is considered to be working. When at least 90% of the power is delivered to the antenna and only 10% of the power is reflected back, this occurs.

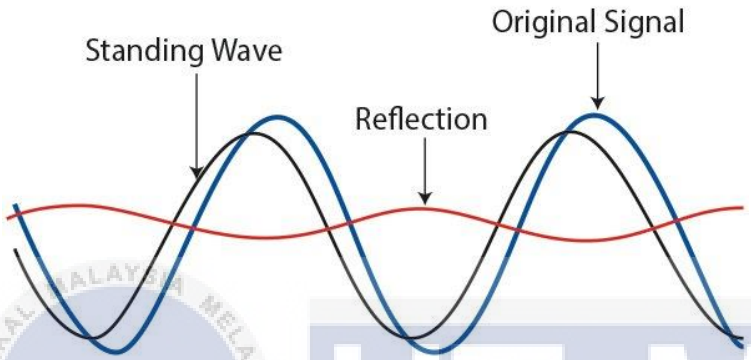

Figure 2.4.1 : Return Loss

2.4.2 Input Impedance

The antenna's input impedance is essentially the impedance it provides at its terminals. It is defined as the voltage to current ratio across the antenna's two input terminals. The antenna impedance is usually expressed as:

$$Z_A = R_A + jX_A$$

In wireless communication, antennas are used to send signals in the form of waves. At the transmitting end, it is designed to convert electrical energy into electromagnetic signals. At the receiving end, the electromagnetic signal is converted to an electrical signal. The transmission line, antenna, and input impedance must all match in order to obtain the highest power transfer. Due to a mismatch between these three parts, a wave will be reflected from the antenna's terminal and returned to the power source, lowering the antenna's efficiency.

2.4.3 Bandwidth

The bandwidth of an antenna is the range of frequencies over which it can operate properly. The bandwidth of a band can be calculated by finding the maximum frequency, minimum frequency, and centre frequency:

BW = 100 x (fH – fL) / fC, where BW is the bandwidth of the antenna.

The maximum frequency is fH.

The minimum frequency is fL.

The central frequency is fC.

The bandwidth is defined as the difference in frequency as a percentage of the bandwidth's centre frequency. Because polarisation, gain, input impedance, and other parameters do not fluctuate in the same way, bandwidth has no distinguishing categorization. As a result, the parameters are determined and set in advance based on the antenna's application.

2.4.4 Gain

Gain is one of the most well-understood antenna parameters, and it is a measurement that incorporates the antenna's efficiency as well as the directional parameter's capabilities. Gain has a lower value than directivity in general. Because gain is defined as the ratio of radiation intensity to input power, this is the case. When compared to a theoretical antenna, antenna gain is the ability of the antenna to radiate more or less in any direction. If you could make an antenna into a perfect sphere, it would radiate evenly in all directions.

2.4.5 Polarization

The direction of the electromagnetic fields created by an antenna when energy radiates away from it is loosely described as the polarisation of the antenna. The direction in which

energy travels away from or is received by an antenna is determined by these directional fields. The polarisation of a wave can then be defined as a wave sent or received by the antenna in a specific direction. A plane wave can be considered to represent a radiated wave at any point in an antenna's far field if its electric-field force is similar to that of a wave whose propagation path coincides with the antenna's radial direction.

There are three types of polarisation: linear, circular, and elliptical. If the vector of an electric field at a point is constantly directed down a line, the field is linearly polarised. The electric field is elliptically polarised if it follows an ellipse-shaped path. Finally, if the ellipse is converted to a circle or a line, the polarisation becomes circular or linear.

2.5 Resonant Frequency

If the SRR is produced on a substrate with a known or unknown dielectric constant, the permittivity of the unknown MUT can be calculated using the relationships between permittivity and dielectric constant. The resonant frequency, f1, of an SRR with a substrate with a known dielectric constant on one side and air on the other can be represented as

$$f_1 \, \alpha \, \frac{1}{\sqrt{\frac{\epsilon_{r1}+1}{2}}}$$

The resonant frequency shifts to when a dielectric sample with an unknown dielectric constant, ϵ_{r2} is placed on the resonator's surface.

$$f_2 \, \alpha \, \frac{1}{\sqrt{\frac{\epsilon_{r1}+\epsilon_{r2}}{2}}}$$

The expression for the MUT unknown dielectric constant as

$$\epsilon_{r2} = \left[\left(\frac{f1}{f2}\right)^2 (\epsilon_{r1} + 1)\right] - \epsilon_{r1}$$

Figure 2.5 shows a plot of ϵ_{r2} and f2 for various MUT with relative permittivity ϵ_{r1}.

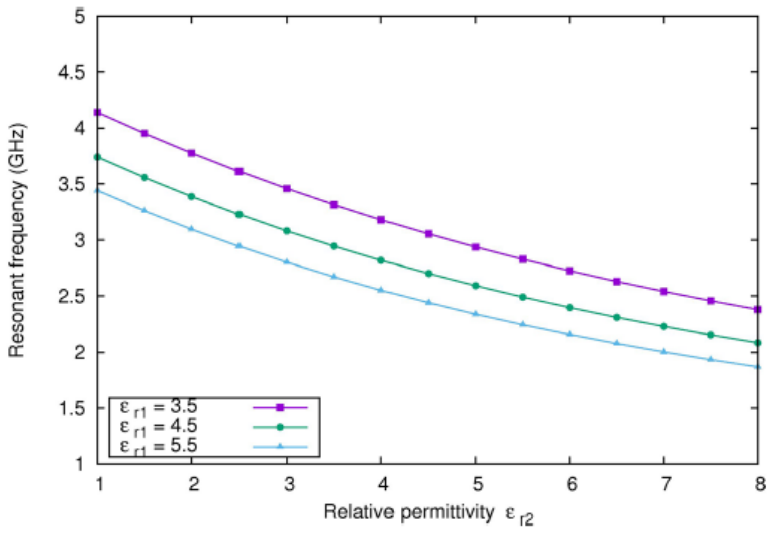

Figure 2.5: Resonant frequency with dielectric constant for different substrate values

When the MUT is used as a sample for the dielectric constant $\in_{r1}$, the resonant frequency can be calculated using the equation.

$$f_2 \, \alpha \, \frac{1}{\sqrt{\in_{r1}}}$$

The dielectric constant of the MUT as

$$\in_{r1} = \left[2\left(\frac{f2}{f1}\right)^2 - 1\right]^{-1}$$

As a result, even without knowing the dielectric constant of the MUT on which the resonator is etched, measuring the dielectric constant of a MUT becomes a simple numerical computation based on the two resonant frequency values f1 and f2.

2.6 Research of Split Ring Resonator

For the past few years, various studies have been conducted on the performance of split ring resonators. These studies were primarily concerned with split ring resonators, return losses,

dielectric constants of various materials, and the various shapes of split ring resonators. Several techniques for designing the split ring resonator are also demonstrated in these studies. The table below summarises different split ring resonator research projects.

Table 3: Research of Split Ring Resonator

Authors(s)	Research Title	Publication Date
Aydin, K., Bulu, I., Guven, K., Kafesaki, M., Soukoulis, C. M., & Ozbay, E.	Investigation of magnetic resonances for different split-ring resonator parameters and designs.	2005
Ayush Jain.	*Split Ring Resonators*	2017, March 31
Pradeep A. S, G. A. Bidkar, Jagadish M.	*Design and Research of Modified Split Ring Resonator for Reduction of Mutual Coupling in Microstrip Patch Antenna Array*.	2019, August
Najuka Hadkar.	*Design of Square Shaped Miniaturized Split Ring Resonators*	2015, May
Ishfaq, M. K.	*Multiband Split-Ring Resonator Based Planar Inverted-F Antenna for 5G Applications*.	2017, March 21
Islam, M. T.	*A Compact Ultrawideband Antenna Based on Hexagonal Split-Ring Resonator for pH Sensor Application*.	2020, July 20
Jagadish, M., & Pradeep, A.	Design of Hexagonal Shaped Split Ring Resonator for Multi-Resonant Behaviour.	2016
Liu, Y.	*Novel Microwave Sensors Based on Split Ring Resonators for Measuring Permittivity*.	2018, May 9
C.Saha, Jwad Y.Siddiqui, Y.M.M. Antar.	*Square Split Ring Resonators: ModellingofResonant Frequency and*	2018, January

	Polarizability.	
Pedro J. Castro Joaquim J. Barroso Joaquim P. Leite Neto A. Tomaz Ugur C. Hasar.	*Experimental Study of Transmission and Reflection Characteristics of a Gradient Array of Metamaterial Split-Ring Resonators*.	2016, October
Vallecchi, A., Shamonina, E., & Stevens, C. J.	Analytical model of the fundamental mode of 3D square split ring resonators.	2019
Xu, K., Liu, Y., Chen, S., Zhao, P., Peng, L., Dong, L., & Wang, G.	Novel Microwave Sensors Based on Split Ring Resonators for Measuring Permittivity.	2018

2.7 Summary

In this chapter, although there are many split ring resonators currently on the market, none of the split ring resonator designs have the characteristics of wide frequency band, high gain, small size and simple structure. Therefore, based on the extensive literature review, it can be concluded that the new design of split ring resonators with SMA ports is a new such technology to be developed. Without any previously developed technology or system as a basis, the task of constructing or inventing a split-ring resonator must start from the hardware structure, system design and implementation.

There are any projects related to ours from other students outside andinside the country. As the world is developing, the use of technologies are widely be used to create and invent a product. The ideas from the previous inventers are being modified and it was make a great come back with improvements. For split ring resonator, not only having previous projects, it also has the commercialized product in the global market. For this product in the market, the usage is wide.

CHAPTER 3

METHODOLOGY

3.1 Introduction

This chapter discuss the methods and procedures, as well as in the entire work process used in the split ring resonator. First, the information about split ring resonator are studied to ensure the project run smoothly and clearly. After getting the information on the proposed title, the project was starting with making split ring resonator has been designed and molded previously. The fluctuation of the resonant frequency was calculated by using related equation. In order to determine the computed and simulated of the split ring resonator, all the related parameters like real part and imaginary part complex permittivity of the split ring resonator are collected and used for the relevant calculation. Then, compare the resonant frequency between three different shape (circle, square, hexagon) and different size of split ring resonator. All results and data were presented in the report. The flow of the project was expressed by using the flow chart of the methodology.

3.2 Research Methodology

3.2.1 Work Flow Block Diagram

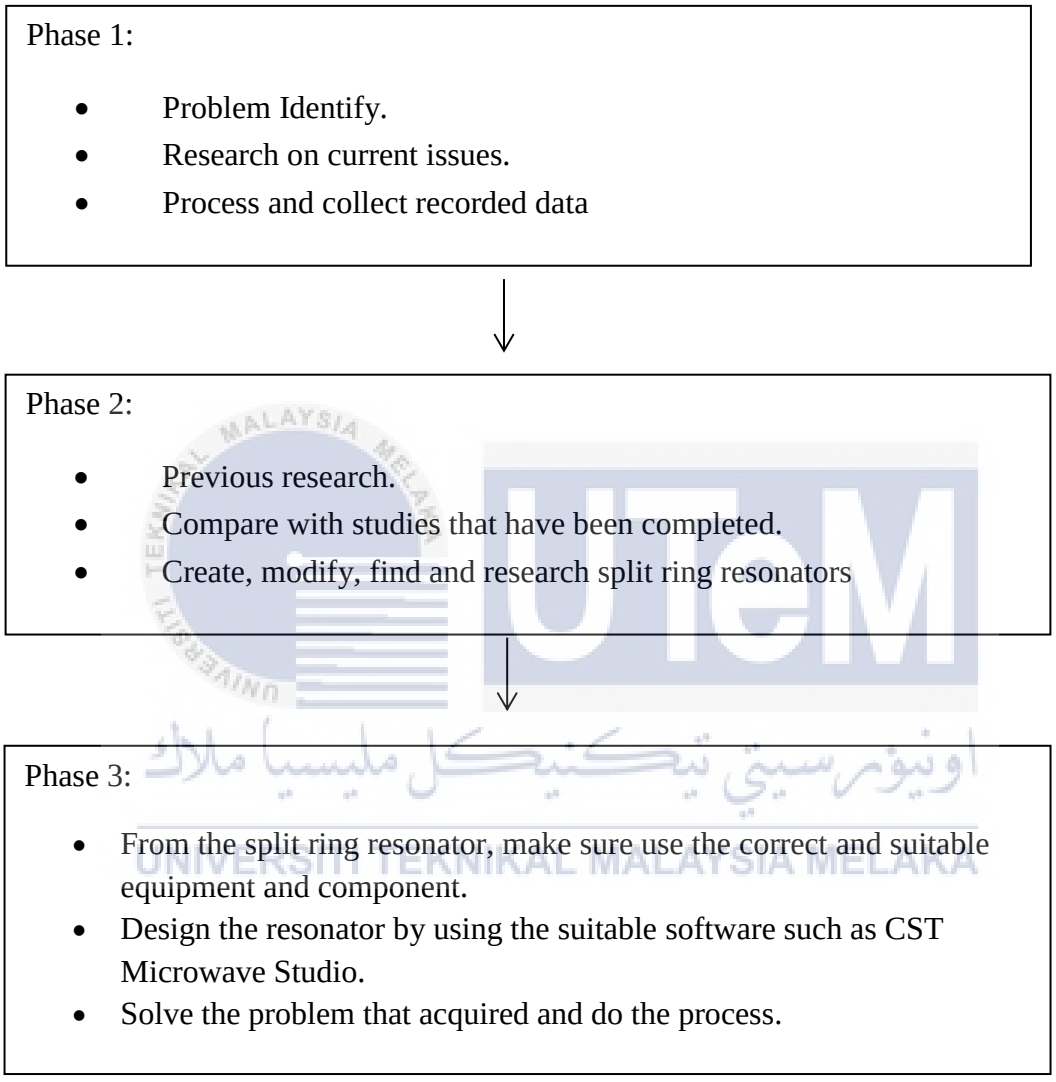

3.2.2 Metamaterials Split Ring Resonators SRR

Circular Ring: Split Ring Resonator Microstip Structure

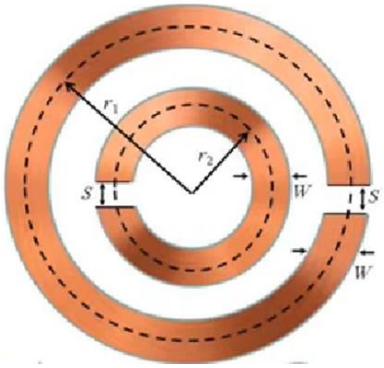

Figure 3.2.2.1: Size of Circular Ring

Average Loop lengths : $L_1 = 2\pi \times r_1 - S$

$L_2 = 2\pi \times r_2 - S$

Resonant frequency of each loop occurs at half-wavelength ($\lambda_g/2$)

$f_1 = \frac{c}{2L_1\sqrt{\varepsilon_{eff}}}$ & $f_2 = \frac{c}{2L_2\sqrt{\varepsilon_{eff}}}$

Square Ring : Split Ring Resonator Microstip Structure

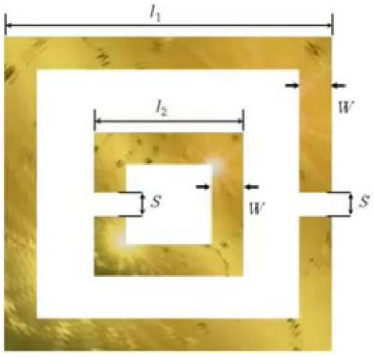

Figure 3.2.2.2: Size of Square Ring

Average Loop lengths : $L_1 = 4 \times l_1 - S - 4 \times W$

$$L_2 = 4 \times l_2 - S - 4 \times W$$

Resonant frequency of each loop occurs at half-wavelength ($\lambda_g/2$)

$f_1 = \frac{c}{2L_1\sqrt{\varepsilon_{eff}}}$ & $f_2 = \frac{c}{2L_2\sqrt{\varepsilon_{eff}}}$

Hexagonal Ring : Split Ring Resonator Microstip Structure

Figure 3.2.2.3: Size of Hexagonal Ring

The hexagonal SRR's Resonant Frequency can be calculated using the equation.

$$f_0 = \frac{1}{(2\pi\sqrt{(2a_{eq}.L_{Net}.C_{Net})})}$$

Where a_{eq} is the Hexagonal SRR's effective radius, and its expression as

$a_{eq} = 2a.\sin(\frac{\pi}{N}) - \frac{g}{N}$

N=6, L_{Net} is the equivalent inductance, and it has the following expression

$L_{Net} = 0.00508 * (2.303 \log_{10}\frac{4l}{c} - 2.636)$

C_{Net} is the structure's equivalent capacitance, and the expression is

$$C_{Net} = \frac{(N.\sin(\frac{\pi}{N})+\beta)^2-(\frac{\Delta}{a})^2}{2(N.\sin(\frac{\pi}{N})+\beta)}$$

3.2.3 Overall Project Methodology

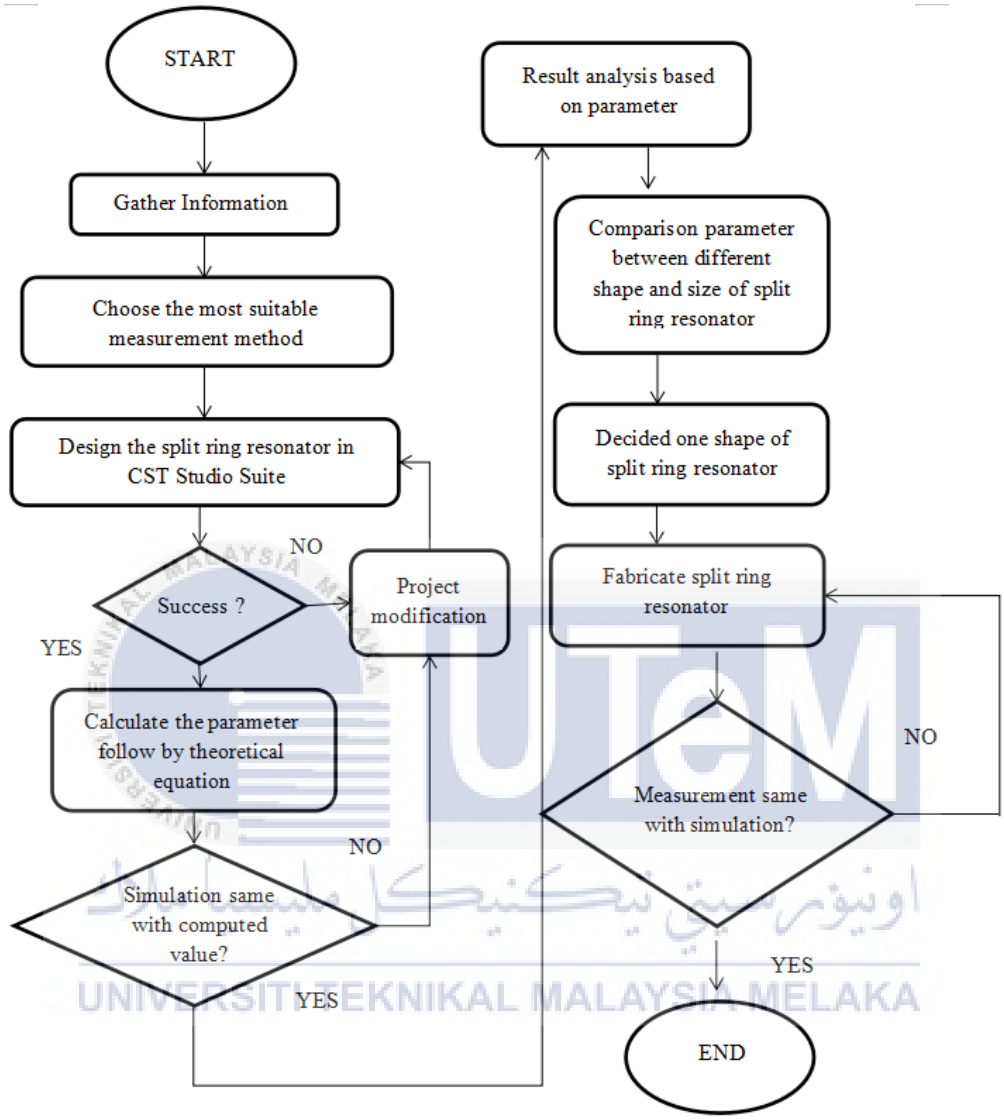

Figure 3.2.3: Flowchart of Methodology

3.3 Software Used

In the project, CST Microwave Studio is used for design and simulation purpose.

3.3.1 CST Microwave Studio

CST Microwave Studio is a professional tool for 3D EM simulation of high frequency (HF) components. CST Microwave Studio can quickly and accurately analyze high frequency (HF) equipment such as planar, filters,antennas, couplers and multilayer structures, and SI and EMC effects. CST software provides time domain and frequency domain solvers, and CST Microwave Studio provides for specific applications can more solver modules. Filters for importing specific CAD files and extracting SPICE parameters can save time and increase design possibilities.

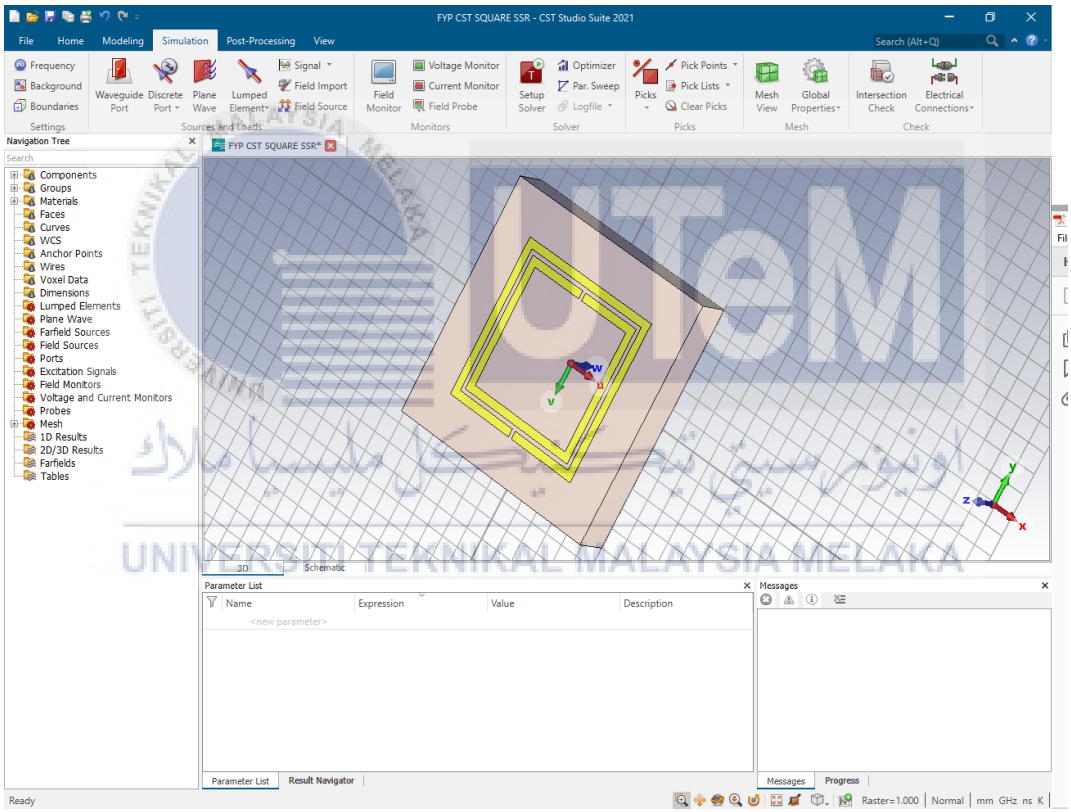

Figure 3.3.1: Split Ring Resoantor design in CST

3.4 Design of SRR

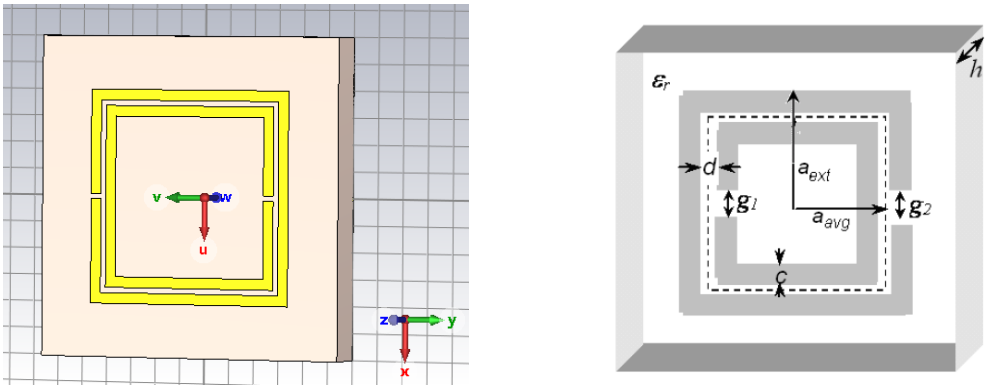

Figure 3.4a: Square Split Ring Resonator

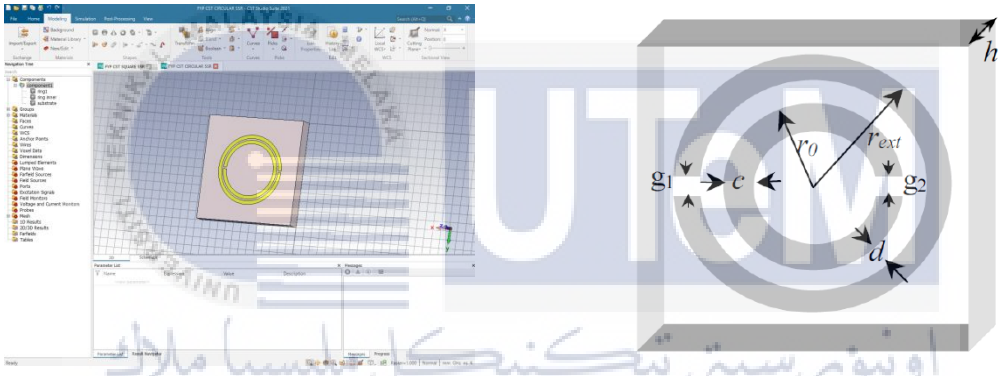

Figure 3.4b: Circular Split Ring Resonator

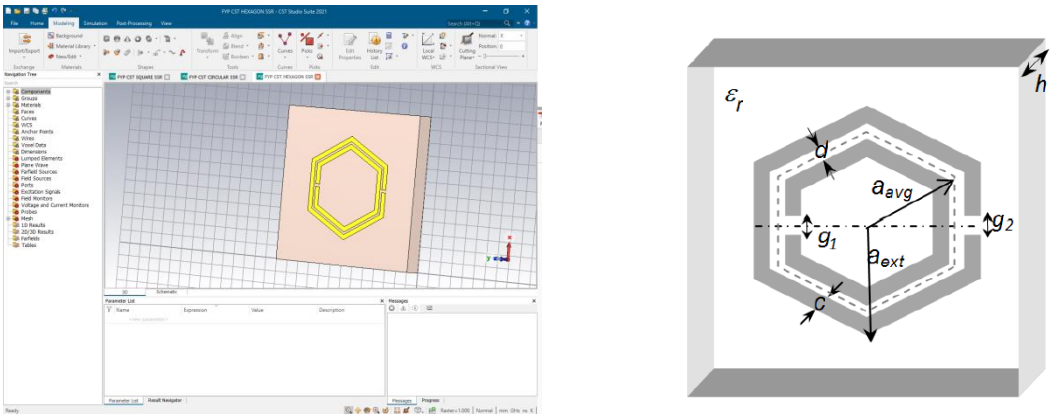

Figure 3.4c: Hexagonal SRR

3.4.1 SRR Resonant Frequency

According to previous discussion, design of split ring resonator by using different shapes (circular, square and hexagon) and different sizes were create a different resonant frequency. Therefore, the resonant frequency of different shapes and sizes of split ring resonator can used to determine the relationship between resonant frequency, sizes and shapes of split ring resonator. Firstly, the resonant frequency of the SRR is given by,

$$\omega_0 = \sqrt{\frac{1}{L_T C_{eq}}}$$

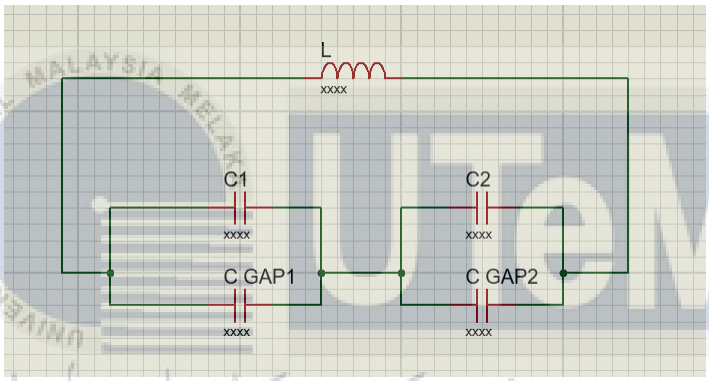

Figure 3.4.1: Equivalent circuit of the SRR show in Figure 3.4

The expression of the resonant frequency of different SRR is given as

For Circular - SRR : $f_{0C} = \frac{1}{2\pi\sqrt{LC_{eq}}} = \frac{1}{2\pi\sqrt{L_T\left[\frac{(\pi r_0 - g)C_{pul}}{2} + \frac{\varepsilon_0 ct}{2g}\right]}}$

For Square - SRR : $f_{0S} = \frac{1}{2\pi\sqrt{L_T C_{eq}}} = \frac{1}{2\pi\sqrt{L_T\left[\left(2a_{avg} - \frac{g}{2}\right)C_{pul} + \frac{\varepsilon_0 ch}{2g}\right]}}$

For Hexagon- SRR : $f_{0H} = \frac{1}{2\pi\sqrt{L_T C_{eq}}} = \frac{1}{2\pi\sqrt{L_T\left[\frac{(3a_{avg} - g_1)C_{pul}}{2} + \frac{\varepsilon_0 ch}{2g_1}\right]}}$

Among them, L_T is the total inductance of split ring resonator, and C_{eq} is the equivalent capacitance of the structure, calculated according to the equivalent circuit in Figure 3.5. C_{pul} is the capacitance per unit length, r_0 (Circular SRR) and a_{avg} (Square SRR and Hexagonal SRR) between the rings are the distance from the center of the two components of the SRR. C_{pul} is calculated as

$$C_{pul} = \frac{\sqrt{\varepsilon_e}}{c_0 Z_0}$$

where $c_0 = 3 \times 10^8$ m/s is speed of light in free space. ε_e is the effective permittivity of the medium and Z_0 is the impedance of the medium. The total inductance of the structures, L_T, is computed as

$$L_T = 0.00508l \left(2.303 \log_{10} \frac{4l}{d} - \boldsymbol{\theta}\right)$$

where, l and d are the wire length and width, respectively. The constant $\boldsymbol{\theta}$ varies with wire geometry and is given as

$\boldsymbol{\theta}$ = 2.45 Circular Split Ring Resonator
= 2.85 for Square Split Ring Resonator
= 2.64 for Hexagonal Split Ring Resonator

3.4.2 Materials Used

Table 4 : The specifications of used SUT materials for sensing

SUT Materials	Permittivity
Roger 5880	2.2
Roger 4350	3.36
FR4	4.4
Roger 3010	11.2 ± 0.3

3.5 Resonant Cavity Method

According to the previous discussion, the method of measuring split-ring resonators using the resonant cavity method is a fairly accurate technique. The deviation of the resonant frequency and the change of the quality factor are determined using this method, which involves loading the cavity resonator with samples. Circular resonators and microstrip line resonators, in addition to resonators, have been employed for this purpose. This method also necessitates meticulous sample processing. To overcome the aforementioned constraints and collect all of the data required to accurately characterise the complicated permittivity of solid materials.

3.6 Split Ring Resonator (FR-4) Fabrication

3.6.1 Printing the Design of Split Ring Resonator

The goal of the previous step of creating films was to sketch out a copper path figure. It's now time to transfer the image from the film to a copper foil.

This step in the split ring resonator manufacturing process prepares the split ring resonator for production. The most basic type of FR-4 double-sided copper plate is a laminate board with epoxy resin as the core material and glass fibre as the substrate material. The copper that constructs the split ring resonator is best received through laminate. The FR-4 has a strong and dust-resistant starting point thanks to the substrate material. Both sides of the copper are pre-bonded. The method entails removing the copper in order to disclose the design from the films.

In FR-4 construction, cleanliness does matter. The copper-sided laminate is cleaned and passed into a decontaminated environment. During this stage, it's vital that no dust particles settle on the laminate. An errant speck of dirt might otherwise cause a circuit to be short or remain open.

Figure 3.6.1 : Exposure Machine

3.6.2 Removing the Unwanted Copper

After removing the picture resist and hardening the resist over the copper we want to maintain, the board moves on to the next step: removing the undesirable copper. A more powerful chemical preparation eats away at the extra copper, just as the alkaline solution did with the resist. All of the exposed copper is removed in the copper solvent solution bath. Meanwhile, beneath the solid layer of photo resist, the desirable copper is completely protected. As a side point, heavier copper boards necessitate more care when it comes to track spacing. The majority of standard FR-4 specifications are comparable. This stage must be done carefully to avoid over-etching; it was etched for about 200 seconds.

The hardened resist protecting the desirable copper needs to be washed off now that the solvent has eliminated the unwanted copper. Another solvent accomplishes this task. The board now glistens with only the copper substrate necessary for the FR-4. After etching, need to stripping process. In this stripping process we want to remove all the excess copper that no need unless track of the circuit.

Figure 3.6.2: Striping

3.6.3 Drying

Board FR-4 put into drying machine to dry up chemical liquid and avoid short circuit.

Figure 3.6.3 : Drying Machine

3.6.4 Cutting

Trim the FR-4 board to the desired size

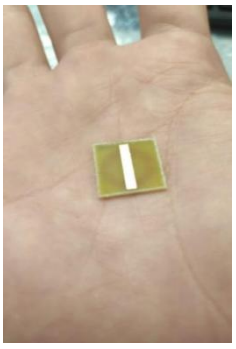

Figure 3.6.4.1 : Bottom View

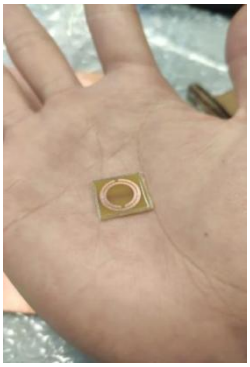

Figure 3.6.4.2 : Top View

3.6.5 Soldering

Soldering the sma port on two side of FR-4 become the connectors

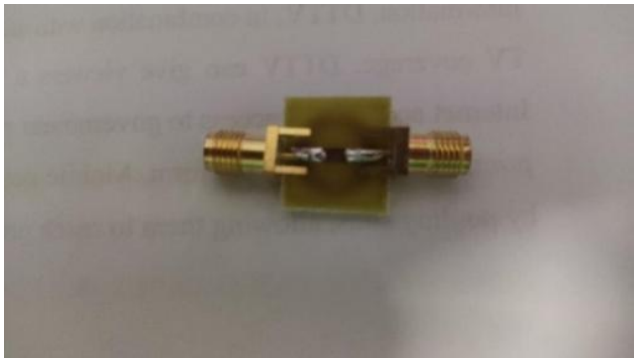

Figure 3.6.5 : Split Ring Resonator After Soldering

3.7 Summary

In this chapter, it can be conclude that the methodology of this project is about frequency resonant calculation, comparison size of split ring resonator and design of split ring resonator. According to the schedule of the project presented in the gantt chart, all the procedures and methods are used and applied to finish this project on time. In Table 5 and 6, it is a gantt chart that shows the schedule of the project. All the data and results are collected and the analysis of the results were discuss in chapter 4.

Table 5 : Gantt Chart of FYP 1

ACTIVITIES / WEEK	1	2	3	4	5	6	7	8	9	10	11	12	13	14
PSM project briefing by supervisor														
Literature review														
Proposal preparation and submission														
Thesis writing chapter 1 and chapter 2														
Design split ring resonator														
Data analysis														
Thesis writing chapter 3, 4 and 5														
Submission of final draft to supervisor														
Preparation of report and presentation														

Table 6 : Gantt Chart of FYP 2

ACTIVITIES / WEEK	1	2	3	4	5	6	7	8	9	10	11	12	13	14
PSM project briefing by supervisor														
Adjust Parameter														
Simulation SRR in CST														
Observation Result														
Fabricate SRR														
Measure SRR by Network Analyzer														
Preparation of report and presentation														

CHAPTER 4

RESULT AND DISCUSSION

4.1 Introduction

This chapter was present about the results of this project. All the result of the split ring resonator based sensor for material characterization were analyzed and discussed. There are resonant frequency, size of split ring resoantor and comparison between three different shape of split ring resonator. Furthermore, the comparison between the shape of split ring resonator and resonant frequency is presented and discussed.

4.2 Resonant Frequency of Three Different Shape of Split Ring Resonator

Simulated resonant frequencies of square SRR, circular SRR and hexagonal SRR for different radius and metallic strips of width, c values are discuss in this part. Parameters: distance between inner ring outer ring, d=0.2mm, split gap g=0.2mm, permittivity εr = 4.4(FR-4), substrate thickness, h =1.575mm. Resonant frequency of SRR of different shape is computed using equations from chapter 3.4.1. The split ring resonator are printed on dielectric substrates having εr =4.4(FR-4) and substrate thickness, h =1.575mm. The resonant frequency was extracted from the transmission coefficient curves when excited by EM wave after simulation. The values were extracted for diameter C-SRR, S-SRR and H-SRR 8 mm and 9mm. For each of these diameter, three different shape ring widths values of the SRR c=0.4mm and 0.5mm are considere.

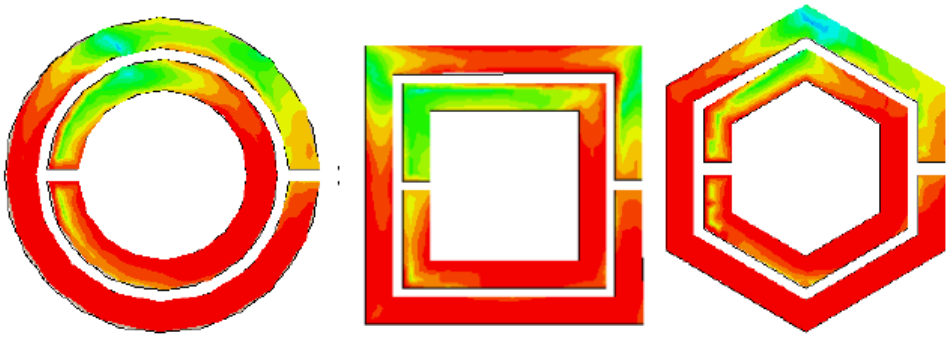

Figure 4.2.1(a): C-SRR Figure 4.2.1(b): S-SRR Figure 4.2.1(c): H-SRR

Comparison of S-parameters between different shape, ring width and diameter of SRR

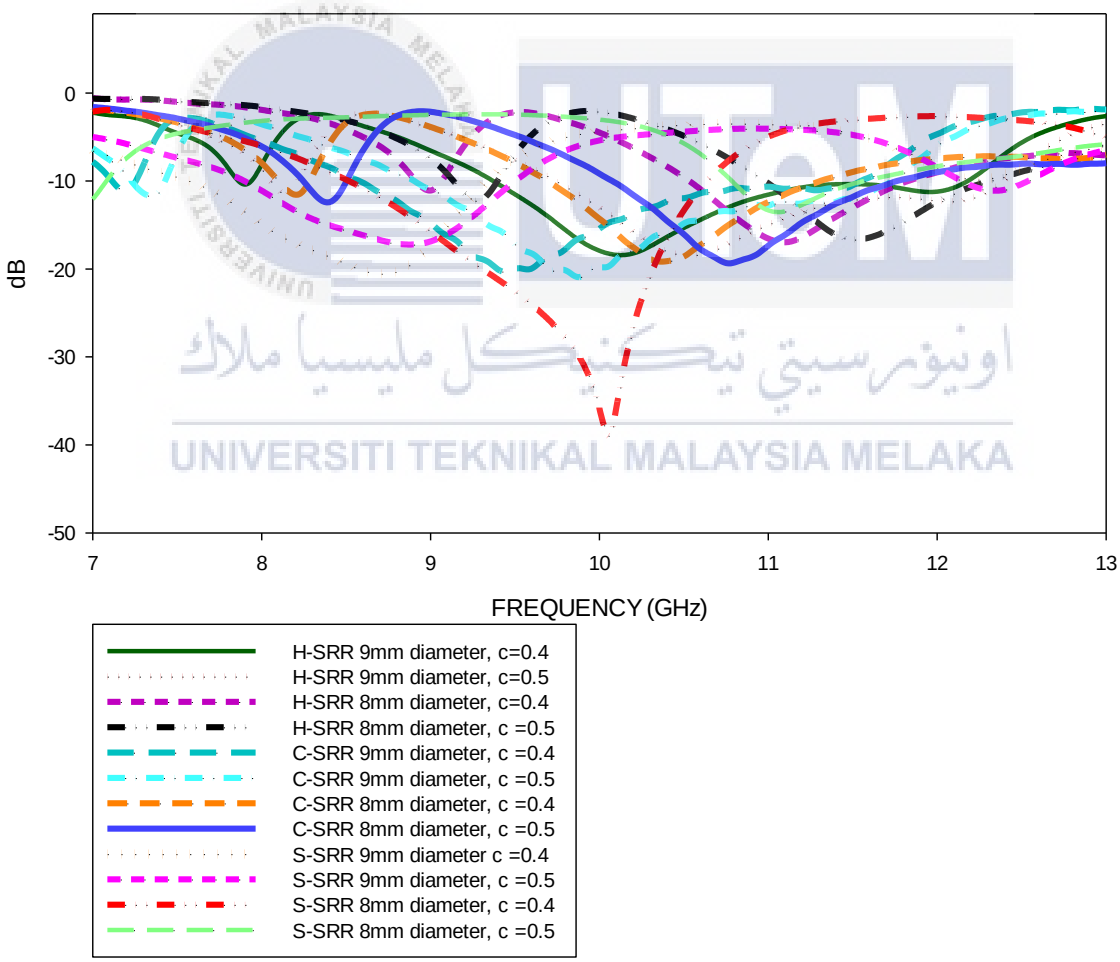

Figure 4.2.2: Comparison of S-parameters between different shape, ring width and diameter of SRR

Figure 4.2.1 shows the different shape of SRR and figure 4.2.2 shows a plot of the simulated resonant frequency as a function of the different ring width *c* as 0.4mm and 0.5mm for all three different shape of SRR.

4.3 Fabricated Antenna

4.3.1 CST Design

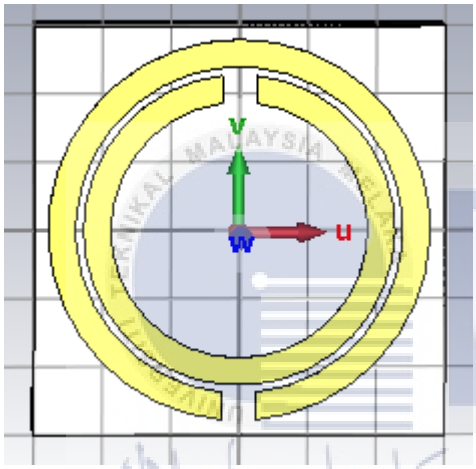

Figure 4.3.1(a): Front design of SRR in CST

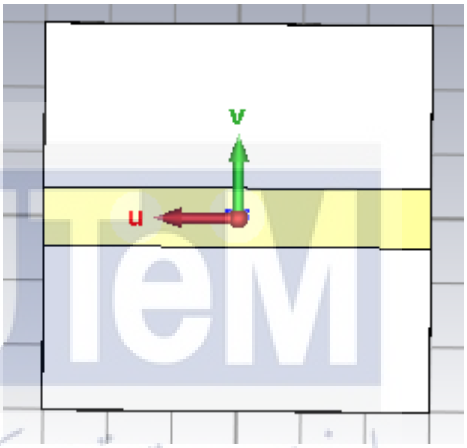

Figure 4.3.1(b): Back design of SRR in CST

4.3.2 Fabricated Design

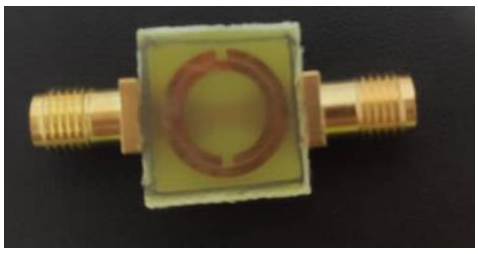

Figure 4.3.2(a): Front design of SRR after fabricate

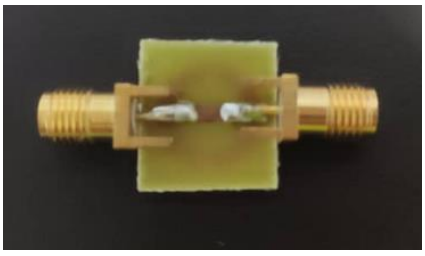

Figure 4.3.2(b): Back design of SRR after fabricate

4.4 Resonant Frequency of Different Gap

Simulated resonant frequencies of square, circular and hexagon of SRR for different split gap dimensions, g are 0.1 mm and 0.4mm are discuss in this part.

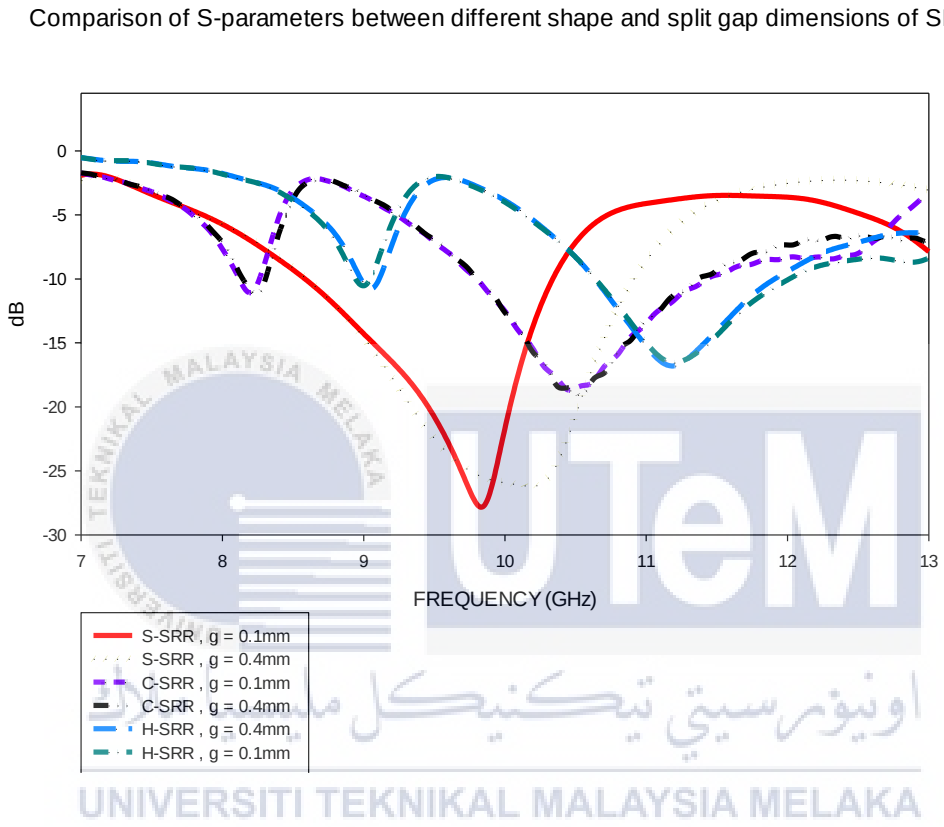

Figure 4.4.1: Comparison of S-parameters between different shape and split gap dimension of SRR

4.5 Parameter List of Split Ring Resonator

Resonant frequency from figure 4.2.2 and 4.4.1 with different shape of split ring resonator, it show the circular split ring resonator was more stable than square split ring resonator and hexagonal split ring resonator. In addition, the difference of resonant frequency of the circular split resonator is smaller than the other two split ring resonators due to the change of the parameter. So the circular split ring resonator was selected from the three shapes.

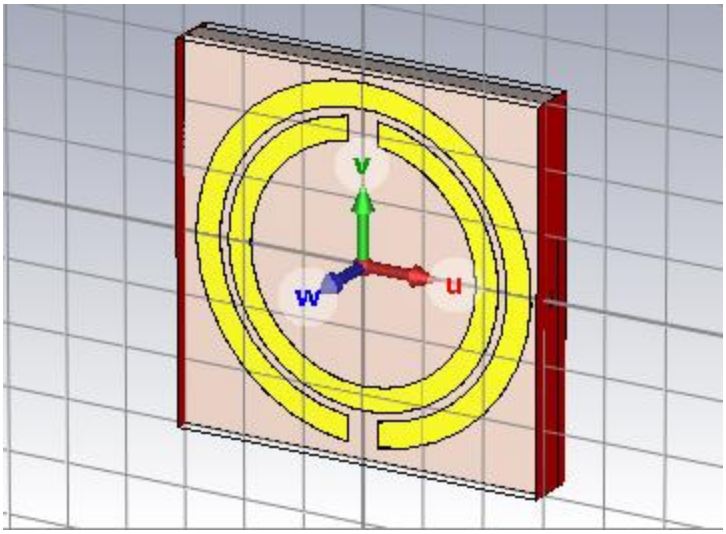

Figure 4.5: Circular Split Ring Resonator

After constant changes and adjustments, the parameter of table 7 was the final parameter of circular split ring resonator. This is because the result of resonant frequency was 3.5GHz and the dB less than -15dB when without placing any MUT on the split ring resonator. According to the theory in chapter 2.4.1, when the dB was greater than -10dB, it mean the function of split ring resonator are considered invalid. In addition, the defects and errors in the process of fabricate FR-4 was cause the results to shift, so it was decided to change the maximum -10dB standard to -15dB, and the 5dB standard was increase success rate of the split ring resonator.

Table 7 : Parameter List of Split Ring Resonator

Name	Value (mm)	Description
g	1.0	Gap
r12	4.78	Inner radius ring 1
r22	3.75	Inner radius ring 2
r21	4.55	Outer radius ring 2
r11	5.58	Outer radius ring 1
h3	0.017	Ring thickness

l	12	Substrate length
h2	0.8	Substrate height
h1	0.035	Wire thickness
a	1.83	Wire width

4.6 Comparison Resonant Frequency and Shift Frequency Between Different Dielectric Constant

Table 8 : Resonant Frequency And Shift Frequency of Different Dielectric Constant

Dielectric Constant	Resonant Frequency (GHz)	Shift Frequency (GHz)
0.5	**3.94**	**3.94 - 3.5 = 0.44**
1.0	**3.86**	**3.86 - 3.5 = 0.36**
1.5	**3.77**	**3.77 - 3.5 = 0.27**
2.0	**3.69**	**3.69 - 3.5 = 0.19**
2.5	**3.62**	**3.62 - 3.5 = 0.12**
3.0	**3.54**	**3.54 - 3.5 = 0.04**
3.5	**3.48**	**3.48 - 3.5 = -0.02**
4.0	**3.42**	**3.42 - 3.5 = -0.08**
4.5	**3.38**	**3.38 - 3.5 = -0.12**
5.0	**3.32**	**3.32 -3.5 = -0.18**
5.5	**3.27**	**3.27 - 3.5 = -0.23**
6.0	**3.22**	**3.22 - 3.5 = -0.28**
6.5	**3.18**	**3.18 - 3.5 = -0.32**

7.0	**3.13**	**3.13 - 3.5 = -0.37**
7.5	**3.09**	**3.09 - 3.5 = -0.41**
8.0	**3.05**	**3.05 - 3.5 = -0.45**
8.5	**3.02**	**3.02 - 3.5 = -0.48**
9.0	**2.97**	**2.97 - 3.5 = -0.53**
9.5	**2.94**	**2.94 - 3.5 = -0.56**
10.0	**2.91**	**2.91 - 3.5 = -0.59**

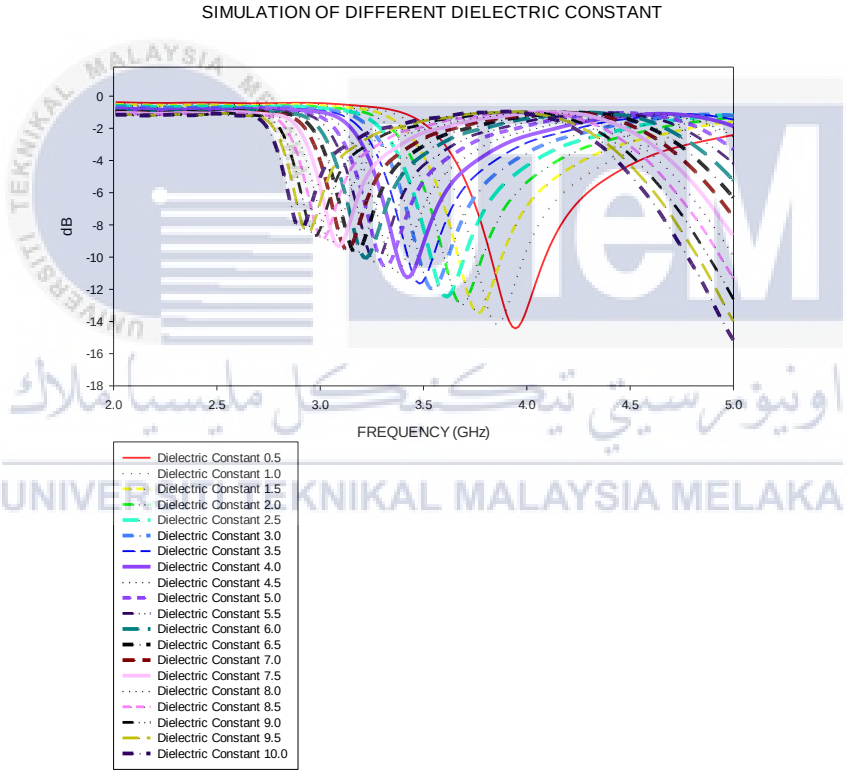

Figure 4.6.1 : Resonant frequency of different dielectric constant

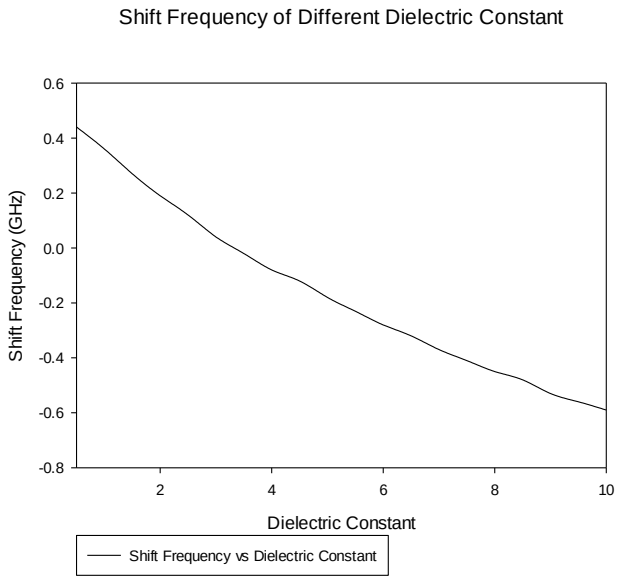

Figure 4.6.2 : Shift frequency of different dielectric constant

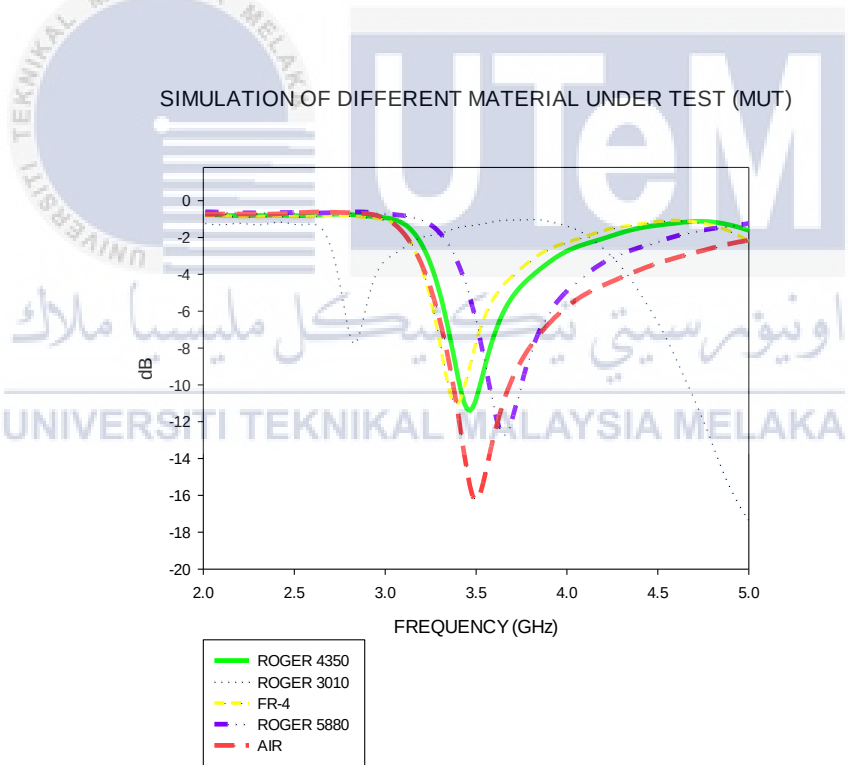

Figure 4.6.3: Resonant frequency of different material under test (MUT)

4.7 Result of Split Ring Resonator

4.7.1 Measure the split ring resonator in lab microwave

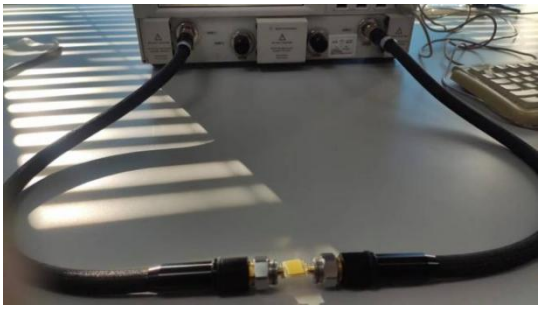

Figure 4.7.1.1: Split ring resonator based sensor test MUT by network analyzer

Figure 4.7.1.2 : Split ring resonator connect with test cable

Figure 4.7.1.3 : Material under test on split ring resonator

4.7.2 Simulation and Measurement of Split Ring Resonator

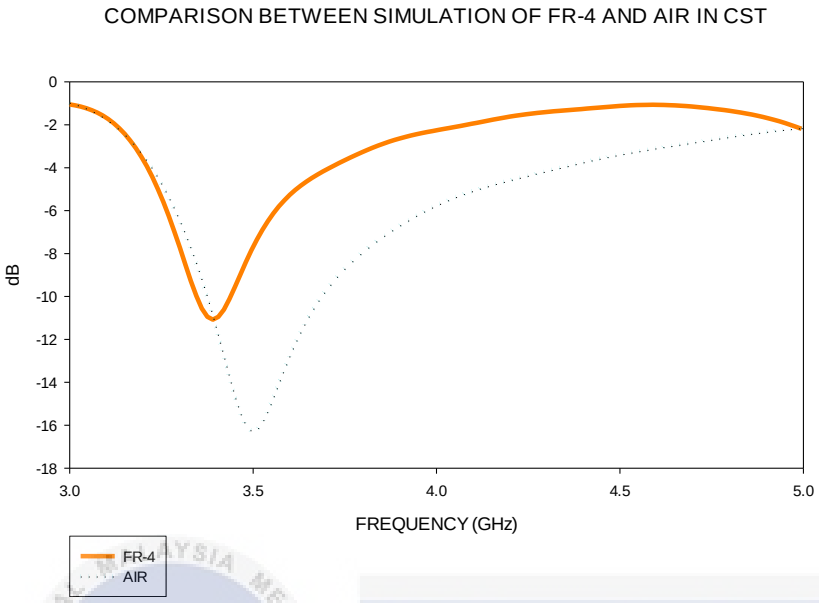

Figure 4.7.2.1 : Comaprison between simulation of FR-4 and air

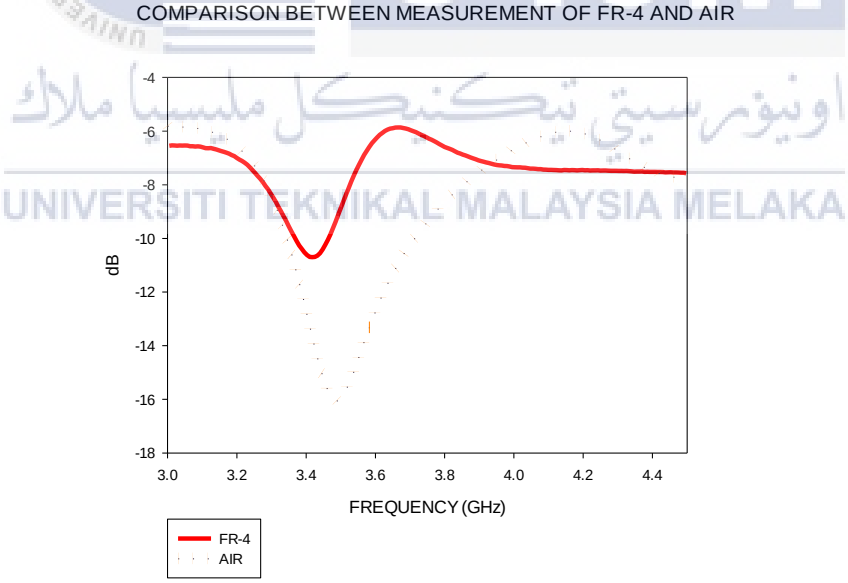

Figure 4.7.2.2 : Comaprison between measurement of FR-4 and air

COMPARISON BETWEEN MEASUREMENT AND SIMULATION OF FR-4 AND AIR

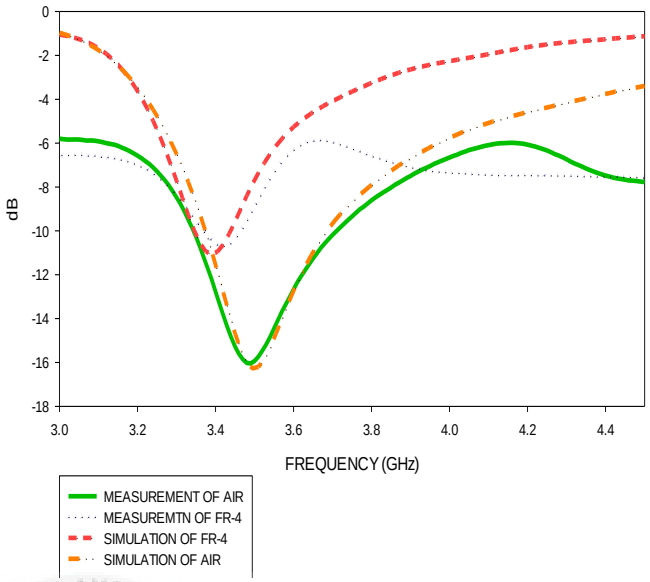

Figure 4.7.2.3 : Comaprison between measurement and simulation of FR-4 and air

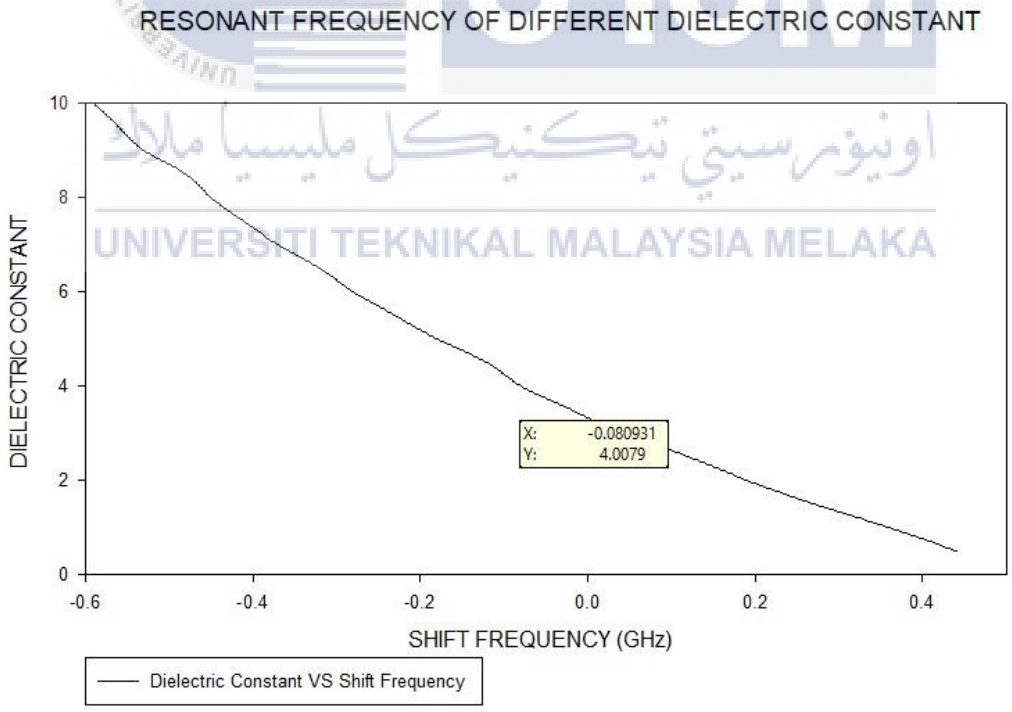

Figure 4.7.2.4: Dielectric constant of shift frequency -0.08

The measurement of FR-4 was 3.42GHz and it shift frequency was -0.08GHz based on equation shift frequency = resonant frequency – 3.5GHz. In figure 4.7.2.4, based on figure 4.6.2 and find out when shift frequency, x was -0.08 and dielectric constant, y was 4.0079, which means 4.0079 was correspond to the table 8 that shift frequency between -0.08 and -0.12. Therefore, dielectric constant of FR-4 was between 4.0 and 4.5. The resonant frequency of both simulation and measurement result is plotted in the same graph as shown in figure 4.7.2.3. Based on figure 4.6.2 the dielectric constant of FR-4 for measurement (4.4) more than simulation result (4.0079) that recorded in figure 4.7.2.4 due to surrounding error. Meanwhile, the measurement result shows that the simulation and measurement are 90.9 percent identical, with 9.09 percent due to errors such as a bad etching procedure or poor soldering skill. Furthermore, the resonant frequency for simulation in figure 4.7.2.1 was slightly same with measurement in figure 4.7.2.2 and the comparison between measurement and simulation was recorded in figure 4.7.2.3.

4.7 Discussion

To achieve the project objectives, the split ring resonator is used in this project. With the consideration of the system losses, the performance resonant frequency of the split ring resonator is included in the circular srr, hexagonal srr and square srr. The resonant frequency is increase directly proportional to the srr metallic strips of width,c and split gap dimensions, g. The different shape (square, hexagonal and circular) and diameter (8mm and 9mm) of split ring resonator are shown in figure 4.2.2 and figure 4.4.1 which show that the resonant frequency of the split ring resonator with different shape and split gap.

For the first time used CST studio suite because it specialist tool for the 3D EM simulation of high frequency components. CST microwave studio enables the fast and accurate analysis of high frequency (HF) devices for split ring resonator. Firstly, design the square, circular and hexagon split ring resonator in CST studio suite software with a FR-4 was used as substrate materials with a dielectric constant of 4.4, copper thickness of 0.017 mm. The project takes SRR as an example to determine metamaterials with strange electromagnetic properties, and analyzes the relationship between the resonant frequency and the equivalent electrical

parameters from the figure 3.4.1 equivalent LC circuit model. In the result of SRR sensor were made of two modified SRR with lateral vertical strips, exhibiting high sensitivity for two resonant frequencies at 7GHz and 13GHz.

Next, in the CST studio suite do the simulation of the split ring resonator and determine the relationship between design of split ring resonator with the resonant frequency. In figure 4.2.1 shows the different shape of the SRR, there are many problems to complete this project such as the resonant frequency of error between different diameter of split ring resonator were big. When simulate the SRR in CST, the radius of C-SRR, S-SRR and H-SRR were designed with 8mm and 9mm. In other hand, metallic strips of width were designed with 0.4mm and 0.5mm. After that, observation the changes of each resonant frequency were recorded in figure 4.2.2. After the simulation done perfectly, the simulated resonant frequency of the each shape of SRR are basically difference. The tabulated comparison shows that for similar footprint with identical diameter values, the S-SRR resonates higher side of the spectrum compared to the H-SRR. The H-SRR resonates higher frequency compared to the C-SRR having similar dimensional parameters, but the resonant frequency of C-SRR was more stable than other shape of design when change the parameter of SRR. Therefore, from figure 4.2.2, the resonant frequency show increased when the value of width ring of SRR increased while the resonant frequency show decreased when the diameter of SRR decreased.

In other hand, the simulated of the SRR for different gap dimensions, g=0.1mm and g=0.4mm were shown in figure 4.4.1. As revealed from figure 4.4.1 depicts the shift in the resonant frequency with S-SRR resonating at higher frequency compared to H-SRR and C-SRR. Based on figure 4.4.1, C-SRR was more stable than H-SRR and S-SRR due to the different of resonant frequency when change the parameter. Furthermore, the resonant frequency were increased when the values of gap, g=0.1mm increase to gap,g=0.4mm in figure 4..4.1.

Furthermore, decided produce the circular split ring resonator as design diagram based on result in figure 4.2.2 and figure 4.4.1. After constant trial and modification, the parameter finally decided to be in table 7. The parameter in table 7 can accurately drop the resonant frequency as 3.5GHz. After having fixed parameters, in figure 4.6.1 was the result that the next process simulate the frequency of material that conduct dielectric constants from 0.5 to 10.0 on split ring resonator based sensor in CST. The resonant frequency and shift frequency that have recorded in

table 8 while figure 4.6.2 were the value of shift frequency and resonant frequency plotted by table 8. In these two graph, that can observe the number of dielectric constant was inversely proportional to shift frequency and resonant frequency.

In figure 4.7.2.1 and figure 4.7.2.2 were the comparison of simulation and measurement between FR-4 and air while figure 4.7.2.3 was combination based on these two figure. In figure 4.7.2.3, the resonant frequency of 3.5 GHz was obtained when don't have MUTs placed on the SRR in the CST. After that, when FR-4 placed on the SRR, an accurate frequency of 3.42 GHz was obtained. In addition, after successfully manufacturing the SRR, it was measured and successfully obtained the same frequency as the result in CST. By comparison simulation and measurement, in figure 4.7.2.3 that show the value of resonant frequency of measurement and simulation were 3.5GHz when don't have put MUT on SRR while in figure 4.7.2.3 also show the value of resonant frequency of measurement and simulation were around 3.42GHz when put FR-4 on SRR. In terms of the operational resonant frequency of FR-4 based on figure 4.7.2.2 different with resonant frequency that showed in figure 4.7.2.4, it can be stated that the simulation result produced the best results when compared to measurement data, which may contain errors such as etching process or bad soldering technique. Unexpected errors can be mitigated or eliminated by practising proper hand-on techniques such as fabrication and cutting. The material had an effect on the simulation as well; in this situation, the substrate must be chosen carefully. The thickness and dielectric constant of the FR-4 substrate provided by FKEKK psm lab differ slightly from the one used in simulation.

4.8 Summary

In this chapter, the different shape, radius and metalic strips of width of split ring resonator, there are different resonant frequency occur and show in figure 4.2.2. In order to find out the relationship between resonant frequency and design circuit, the different gap of SRR were designed and result recorded in figure 4.4.1. Moreover, the different dielectric constant there are different shift frequency and resonant frequency occur and shown in table 8. In figure 4.7.2.3, the simulation and measurement almost same. Resonant frequency was 3.5GHz when don't put any material on SRR while resonant frequency was 3.42GHz when put the FR-4 on SRR.

CHAPTER 5

CONCLUSION AND RECOMMENDATION

5.1 Conclusion

In conclusion, all objective for this project had been achieved. Resonant frequency of split ring resonator was completely simulated in CST. With this project, split ring resonator is suitable to be used in such circuits, due to its electrical properties and smaller foot print. A simplified equivalent circuit model is used to explain the microwave sensor's design, and a very good agreement between the circuit model and the full electromagnetic simulation results is achieved. In the recent years, the split ring resonator technology has become popular as it can capability to modify the resonant frequency by altering the structure, the user can change the resonant frequency depends on the design of SRR. From the result, S-SRR can generate resonant frequency higher than H-SRR while H-SRR can generate resonant frequency higher than C-SRR. The resonant frequency was change caused by the different design of SRR while resonant frequency also was change caused by the different value dielectric constant of MUT. Furthermore, simulation and measurement were almost same, the hardware of split ring resonator were successful determine the accurate measurement for complex permittivity of materials and the design of split ring resonator based sensor can accurate complex permittivity measurements of solid dielectrics. Finally, in this project, learned the all of the SRR function and know the weakness of the each SRR, and also learned the ways to solve the problem that faced for completed this project. At the end, all the simulation and measurement obtained were accurate and completed.

5.2 Recommendation for Future Work

Based on this final year project 2, had done the simulation and measurement about split ring resonator. First of all, as a degree student, had known how to develop design process and the workflow for final year project 2. During this completing process of the project, time is very important especially to make sure that the split ring resonator can be function and completely done at the given time in nearly work. Student had make sure that was followed the time management so that the project can be done. From this project, the recommendation in further research is the improvement on the simulation and measurement of SRR in CST and hardware that can get the more accurate value and increase the type of MUT. The measurement should measure for the different value of diameter, ring widths, split gap dimensions of SRR and more different type of material to obtain a better observation on the resonant frequency. With more data measurement, the SRR determination can be more precise and accurate. Besides that, the application of SRR should be carry out. By doing the real application, all the results are useful and can be used for further research. Moreover, investigate SRR can be used to measure the permeability for magnetic samples and if a lower losses substrate will improve the results.

REFERENCES

[1] A free-space method for measurement of dielectric constants and loss tangents at microwave frequencies. (1989, June 1). IEEE Journals & Magazine | IEEE Xplore. https://ieeexplore.ieee.org/document/32194

[2] Analysis, C. S. (2021, March 16). *Single Split-Ring Resonator Design*. Cadence. https://resources.system-analysis.cadence.com/blog/msa2021-single-split-ring-resonator-design

[3] Aydin, K., Bulu, I., Guven, K., Kafesaki, M., Soukoulis, C. M., & Ozbay, E. (2005). Investigation of magnetic resonances for different split-ring resonator parameters and designs. *New Journal of Physics*, *7*, 168. https://doi.org/10.1088/1367-2630/7/1/168

[4] Ayush Jain. (2017b, March 31). *Split Ring Resonators* [Video]. YouTube. https://www.youtube.com/watch?v=WkbgU6Zr_WM

[5] CST and HFSS Antenna & Metamatarial Designing. (2020, April 22). *How to design polarization conversion metamatarial in cst in English* [Video]. YouTube. https://www.youtube.com/watch?v=KN3XYbxe9w0

[6] EMMINES. (2014, December 4). *Metamaterial Unit cell Square SRR design using CST and HFSS part 1* [Video]. YouTube. https://www.youtube.com/watch?v=DxXR_hyDR1Q

[7] EMMINES. (2014b, December 4). *Metamaterial Unit cell Square SRR design using CST and HFSS part 2* [Video]. YouTube. https://www.youtube.com/watch?v=BuObryXXlXg&t=163s

[8] Fan. (2019, June 3). *mm-Wave Ring Resonator* [Video]. YouTube. https://www.youtube.com/watch?v=nvknTtH1BFk

[9] Hwan Kim, J., Seob Kang, J., II Park, J., & Weon Kang, T. (2014, June). A new method for the determination of the reflection and transmission characteristics of dielectric materials. A New Method for the Determination of the Reflection and Transmission Characteristics of Dielectric Materials. https://doi.org/10.1109/ARFTG.2014.6899536

[10] ijera. (2015, May). *Design of Square Shaped Miniaturized Split Ring Resonators*. Najuka Hadkar. http://www.ijera.com/papers/Vol5_issue5/Part%20-%204/C55041114.pdf

[11] IJEAT. (2019, August). *Design and Research of Modified Split Ring Resonator for Reduction of Mutual Coupling in Microstrip Patch Antenna Array*. Pradeep A. S, G. A. Bidkar, Jagadish M. https://www.ijeat.org/wp-content/uploads/papers/v8i6/F9375088619.pdf

[12] Ishfaq, M. K. (2017, March 21). *Multiband Split-Ring Resonator Based Planar Inverted-F Antenna for 5G Applications*. Hindawi. https://www.hindawi.com/journals/ijap/2017/5148083/

[13] Islam, M. T. (2018, July 20). *A Compact Ultrawideband Antenna Based on Hexagonal Split-Ring Resonator for pH Sensor Application*. MDPI. https://www.mdpi.com/1424-8220/18/9/2959/htm

[14] Ismael Azeez, H., Shan Chen, W., Kuang Wu, C., Min Cheng, C., & Chi Yang, H. (2018, January). A Simple Resonance Method to Investigate Dielectric Constant of Low Loss Substrates for Smart Clothing. https://myukk.org/SM2017/sm_pdf/SM1522.pdf

[15] Jagadish, M., & Pradeep, A. (2016). Design of Hexagonal Shaped Split Ring Resonator for Multi-Resonant Behaviour. *Bonfring International Journal of Research in Communication Engineering*, *6*(Special Issue), 20–23. https://doi.org/10.9756/bijrce.8193

[16] Liu, Y. (2018, May 9). *Novel Microwave Sensors Based on Split Ring Resonators for Measuring Permittivity*. IEEE Journals & Magazine | IEEE Xplore. https://ieeexplore.ieee.org/document/8356624?denied=

[17] ResearchGate. (2018, January). *Square Split Ring Resonators: ModellingofResonant Frequency and Polarizability*. C.Saha, Jwad Y.Siddiqui, Y.M.M. Antar. https://www.researchgate.net/publication/224332556_Square_Split_Ring_Resonators_Modelling_of_resonant_frequency_and_polarizability

[18] scielo brazil. (2016, October). *Experimental Study of Transmission and Reflection Characteristics of a Gradient Array of Metamaterial Split-Ring Resonators*. Pedro J. Castro Joaquim J. Barroso Joaquim P. Leite Neto A. Tomaz Ugur C. Hasar. https://www.scielo.br/j/jmoea/a/mNTyTzTsg9gKbdKpgYwgMVH/?lang=en

[19] Vallecchi, A., Shamonina, E., & Stevens, C. J. (2019). Analytical model of the fundamental mode of 3D square split ring resonators. *Journal of Applied Physics*, *125*(1), 014901. https://doi.org/10.1063/1.5053482

[20] Wang, J. (2020, October 6). Open-Ended Coaxial Cable Selection for Measurement of Liquid Dielectric Properties via the Reflection Method. Hindawi. https://www.hindawi.com/journals/mpe/2020/8942096/

[21] Xu, K., Liu, Y., Chen, S., Zhao, P., Peng, L., Dong, L., & Wang, G. (2018). Novel Microwave Sensors Based on Split Ring Resonators for Measuring Permittivity. *IEEE Access*, *6*, 26111–26120. https://doi.org/10.1109/access.2018.2834726

APPENDICES

Appendix A: LIST OF DIELECTRIC MATERIALS AND PROPERTIES

S. No.	Dielectric Material	Relative Permittivity	Loss Tangent
1	Air	1.0006	0
2	FR4 epoxy	4.4	0.02
3	Bakelite	4.8	0.0002
4	Duroid	2.2	0.0009
5	Quartz glass	3.78	0
6	Foam	1.03	0
7	Polystyrene	2.55	0
8	Plexiglas	2.59	0.0068
9	Fused quartz	3.78	0
10	E glass	6.22	0.0023
11	RO4725JXR	2.55	0.0022
12	RO4730JXR	3	0.0023
13	Rogers RT/duroid 5870/5880	2.33/2.2	0.0012/0.0009
14	Teflon	2.1	0.001
15	Taconic CER-10	10	0.0035
16	Taconic RF-30	3	0.0014
17	Taconic RF-35	3.5	0.0018

Appendix B: FR-4 DATA SHEET

Laminate Requirements		Thickness < 0,50mm		Thickness ≥ 0,5mm		Units	Test Method
		Typical Value	Specification	Typical Value	Specification	Metric	IPC-TM-650 or as described
Peel Strength, minimum	A: Low profile copper foil and very low profile copper foil – all copper foil > 17µm	0,9	0,70	0,95	0,70		2.4.8
	B: Standard profile copper foil						
	1. After thermal stress	1,05	0,80	1,20	1,05	N/mm	2.4.8.2
	2. At 125°C	0,95	0,70	1,15	0,70		2.4.8.3
	3. After process solutions	0,8	0,55	1,0	0,80		2.4.8
	C: All other foil - composite		AABUS		AABUS		
Volume Resistivity, minimum	A: C-96/35/90	$4\ 10^6$	10^6	$6\ 10^6$			
	B: After humidity conditioning			$4\ 10^8$	10^6	MΩ cm	2.5.17.1
	C: At elevated temperature E-24/125	$7\ 10^5$	10^3	$7\ 10^5$	10^3		
Surface Resistivity, minimum	A: C-96/35/90	$1\ 10^6$	10^4				
	B: After humidity conditioning			$3\ 10^5$	10^4	MΩ	2.5.17.1
	C: At elevated temperature E-24/125	$6\ 10^5$	10^3	$6\ 10^5$	10^3		
Moisture Absorption, maximum		0,4		0,4	0,80	%	
Dielectric Breakdown, minimum				45	40	kV	2.5.6
Permittivity @ 1MHz (Laminate and prepreg as laminated)		4,2-4,6	5,4	4,6-4,9	5,4		2.5.5.2 2.5.5.3 2.5.5.9
Loss Tangent @ 1MHz (Laminate and prepreg as laminated)		0,015-0,02	0,035	0,015-0,02	0,035		2.5.5.2 2.5.5.3 2.5.5.9
Flexural Strength , minimum	A: Length direction			440	415	N/mm^2	2.4.4
	B: Cross direction			400	345		
Arc Resistance, minimum		105	60	105	60	s	2.5.1
Thermal Stress 10 s @288°C, minimum	Unetched	Pass	Pass Visual	Pass	Pass Visual	rating	2.4.13.1
	Etched	Pass	Pass Visual	Pass	Pass Visual		
Electric Strength, minimum (Laminate and prepreg as laminated)		39	30			kV/mm	2.5.6.2
Flammability (Laminate and prepreg as laminated)		V0	min. V0	V0	min. V0	rating	UL94
Halogen content , maximum	Chlor	-		-		ppm	2.3.41
	Brom	-		-			
	Chlor + Brom	-		-			
Glass Transition Temperature				135	min. 110	°C	2.4.24
Decomposition Temperature			-	310	-	°C	2.4.24.6 (5% weight loss)
CTE Z-axis	A: Alpha 1		-		-	ppm/°C	
	B: Alpha 2		-		-	ppm/°C	2.4.24
	C: 50°C – 260°C		-	3,8-4,2	-	%	
Time to Delamination (TMA) (copper removed)	A: T260		-	15	-		2.4.24.1 and corresponding adjustments in 3.10.1.2
	B: T288		-		-	Minutes	
	C: T300		-		-		
Others							
PLC				3		Class	UL
CTI				200	175 - 250	V	IEC 112

Appendix C: ROGER 5870 AND 5880 DATA SHEET

	RT/duroid 5870		RT/duroid 5880					
[1]Dielectric Constant, ε_r Process	2.33 2.33 ± 0.02 spec.		2.20 2.20 ± 0.02 spec.		Z Z	N/A	C24/23/50 C24/23/50	1 MHz IPC-TM-650 2.5.5.3 10 GHz IPC-TM 2.5.5.5
[4]Dielectric Constant, ε_r Design	2.33		2.20		Z	N/A	8 GHz - 40 GHz	Differential Phase Length Method
Dissipation Factor, tan δ	0.0005 0.0012		0.0004 0.0009		Z Z	N/A	C24/23/50 C24/23/50	1 MHz IPC-TM-650, 2.5.5.3 10 GHz IPC-TM-2.5.5.5
Thermal Coefficient of ε_r	-115		-125		Z	ppm/°C	-50 - 150°C	IPC-TM-650, 2.5.5.5
Volume Resistivity	2 X 10^7		2 X 10^7		Z	Mohm cm	C96/35/90	ASTM D257
Surface Resistivity	2 X 10^7		3 X 10^7		Z	Mohm	C/96/35/90	ASTM D257
Specific Heat	0.96 (0.23)		0.96 (0.23)		N/A	J/g/K (cal/g/C)	N/A	Calculated
Tensile Modulus	Test at 23 °C	Test at 100 °C	Test at 23 °C	Test at 100 °C	N/A	MPa (kpsi)	A	ASTM D638
	1300 (189)	490 (71)	1070 (156)	450 (65)	X			
	1280 (185)	430 (63)	860 (125)	380 (55)	Y			
ultimate stress	50 (7.3)	34 (4.8)	29 (4.2)	20 (2.9)	X			
	42 (6.1)	34 (4.8)	27 (3.9)	18 (2.6)	Y			
ultimate strain	9.8	8.7	6.0	7.2	X	%		
	9.8	8.6	4.9	5.8	Y			
Compressive Modulus	1210 (176)	680 (99)	710 (103)	500 (73)	X	MPa (kpsi)	A	ASTM D695
	1360 (198)	860 (125)	710 (103)	500 (73)	Y			
	803 (120)	520 (76)	940 (136)	670 (97)	Z			
ultimate stress	30 (4.4)	23 (3.4)	27 (3.9)	22 (3.2)	X			
	37 (5.3)	25 (3.7)	29 (5.3)	21 (3.1)	Y			
	54 (7.8)	37 (5.3)	52 (7.5)	43 (6.3)	Z			
ultimate strain	4.0	4.3	8.5	8.4	X	%		
	3.3	3.3	7.7	7.8	Y			
	8.7	8.5	12.5	17.6	Z			
Moisture Absorption	0.02		0.02		N/A	%	.062" (1.6mm) D48/50	ASTM D570
Thermal Conductivity	0.22		0.20		Z	W/m/K	80°C	ASTM C518
Coefficient of Thermal Expansion	22 28 173		31 48 237		X Y Z	ppm/°C	0-100°C	IPC-TM-650, 2.4.41
Td	500		500		N/A	°C TGA	N/A	ASTM D3850
Density	2.2		2.2		N/A	gm/cm³	N/A	ASTM D792
Copper Peel	27.2 (4.8)		31.2 (5.5)		N/A	pli (N/mm)	1 oz (35mm) EDC foil after solder float	IPC-TM-650 2.4.8
Flammability	V-0		V-0		N/A	N/A	N/A	UL94
Lead-Free Process Compatible	Yes		Yes		N/A	N/A	N/A	N/A

Appendix D: ROGER 4003C AND 4390B DATA SHEET

Property	Typical Value RO4003C	Typical Value RO4350B	Direction	Units	Condition	Test Method
Dielectric Constant, ε_r Process	3.38 ± 0.05	[1] 3.48 ± 0.05	Z	--	10 GHz/23°C	IPC-TM-650 2.5.5.5 Clamped Stripline
[2] Dielectric Constant, ε_r Design	3.55	3.66	Z	--	8 to 40 GHz	Differential Phase Length Method
Dissipation Factor tan, δ	0.0027 0.0021	0.0037 0.0031	Z	--	10 GHz/23°C 2.5 GHz/23°C	IPC-TM-650 2.5.5.5
Thermal Coefficient of ε_r	+40	+50	Z	ppm/°C	-50°C to 150°C	IPC-TM-650 2.5.5.5
Volume Resistivity	1.7 X 10^{10}	1.2 X 10^{10}		MΩ•cm	COND A	IPC-TM-650 2.5.17.1
Surface Resistivity	4.2 X 10^{9}	5.7 X 10^{9}		MΩ	COND A	IPC-TM-650 2.5.17.1
Electrical Strength	31.2 (780)	31.2 (780)	Z	KV/mm (V/mil)	0.51mm (0.020")	IPC-TM-650 2.5.6.2
Tensile Modulus	19,650 (2,850) 19,450 (2,821)	16,767 (2,432) 14,153 (2,053)	X Y	MPa (ksi)	RT	ASTM D638
Tensile Strength	139 (20.2) 100 (14.5)	203 (29.5) 130 (18.9)	X Y	MPa (ksi)	RT	ASTM D638
Flexural Strength	276 (40)	255 (37)		MPa (kpsi)		IPC-TM-650 2.4.4
Dimensional Stability	<0.3	<0.5	X,Y	mm/m (mils/inch)	after etch +E2/150°C	IPC-TM-650 2.4.39A
Coefficient of Thermal Expansion	11 14 46	10 12 32	X Y Z	ppm/°C	-55 to 288°C	IPC-TM-650 2.4.41
Tg	>280	>280		°C TMA	A	IPC-TM-650 2.4.24.3
Td	425	390		°C TGA		ASTM D3850
Thermal Conductivity	0.71	0.69		W/m/°K	80°C	ASTM C518
Moisture Absorption	0.06	0.06		%	48 hrs immersion 0.060" sample Temperature 50°C	ASTM D570
Density	1.79	1.86		gm/cm³	23°C	ASTM D792
Copper Peel Strength	1.05 (6.0)	0.88 (5.0)		N/mm (pli)	after solder float 1 oz. EDC Foil	IPC-TM-650 2.4.8
Flammability	N/A	[3] V-0				UL 94
Lead-Free Process Compatible	Yes	Yes				

Appendix E: CHINA MADE HIGH FREQUENCY SUBSTRATE F4B DATA SHEET

PCB Specifications	
Layer count:	Double sided
Base material:	F4B DK 2.2
Dimension:	25 x 26mm
Finished thickness	3.0mm ±10%
Finished Copper weight:	1oz
SMOBC:	No
Surface finish:	HASL Pb free

PCB Capability	
PCB Material:	PTFE
Code:	F4B series
Dielectric constant:	2.2, 2.55 and 2.65
	2.17, 2.45, 2.75 and 3.0
Layer count:	1 Layer, 2 Layer, Multilayer, Hybrid type
Copper weight:	0.5oz, 1oz, 2oz, 3oz
PCB thickness:	0.17mm, 0.25mm, 0.5mm, 0.8mm, 1.0mm,
	1.5mm, 2.0mm, 3.0mm, 4.0mm and 5.0mm, etc.
PCB Size:	≤400mm X 500mm
Surface finish:	Bare copper, HASL, ENIG, Immersion tin etc.

Appendix F: ROGER 3010 DATA SHEET

Property	Typical Value[1]				Direction	Unit	Condition	Test Method
	RO3003	RO3035	RO3006	RO3010				
Dielectric Constant, ε_r Process	3.00 ± 0.04	3.50 ± 0.05	6.15 ± 0.15	10.2 ± 0.30	Z	-	10 GHz 23°C	IPC-TM-650 2.5.5.5 Clamped Stripline
[2] Dielectric Constant, ε_r Design	3.00	3.60	6.50	11.20	Z	-	8 GHz - 40 GHz	Differential Phase Length Method
Dissipation Factor, tan δ	0.0010	0.0015	0.0020	0.0022	Z	-	10 GHz 23°C	IPC-TM-650 2.5.5.5
Thermal Coefficient of ε_r	-3	-45	-262	-395	Z	ppm/°C	10 GHz -50 to 150°C	IPC-TM-650 2.5.5.5
Dimensional Stability	-0.06 0.07	-0.11 0.11	-0.27 -0.15	-0.35 -0.31	X Y	mm/m	COND A	IPC TM-650 2.2.4
Volume Resistivity	10^7	10^7	10^5	10^5		MΩ•cm	COND A	IPC 2.5.17.1
Surface Resistivity	10^7	10^7	10^5	10^5		MΩ	COND A	IPC 2.5.17.1
Tensile Modulus	930 823	1025 1006	1498 1293	1902 1934	X Y	MPa	23°C	ASTM D638
Moisture Absorption	0.04	0.04	0.02	0.05	-	%	D48/50	IPC-TM-650 2.6.2.1
Specific Heat	0.9		0.86	0.8		J/g/K		Calculated
Thermal Conductivity	0.50	0.50	0.79	0.95	-	W/m/K	50°C	ASTM D5470
Coefficient of Thermal Expansion (-55 to 288 °C)	17 16 25	17 17 24	17 17 24	13 11 16	X Y Z	ppm/°C	23°C/50% RH	IPC-TM-650 2.4.41
Td	500	500	500	500		°C TGA		ASTM D3850
Density	2.1	2.1	2.6	2.8		gm/cm³	23°C	ASTM D792
Copper Peel Strength	12.7	10.2	7.1	9.4		lb/in	1 oz. EDC After Solder Float	IPC-TM-2.4.8
Flammability	V-0	V-0	V-0	V-0				UL 94
Lead Free Process Compatible	YES	YES	YES	YES				